Pregnancy Reduces COVID-19 Vaccine Immunity Against Novel Variants

Maclaine A. Parish[1], Jaiprasath Sachithanandham[1], Lizeth Gutierrez[2], Han-Sol Park[1], Anna Yin[1], Katerina Roznik[2], Patrick Creisher[1], John S. Lee[1], Laura A. St Clair, [1] Annie Werner[1], Susan Bersoff-Matcha[3], Catherine Pilgrim-Grayson[4], Lea Berhane[4], Hana Golding[5], Patrick Shea[1], Katherine Fenstermacher[6], Richard Rothman[6], Irina Burd[7], Jeanne Sheffield[8], Andrea L. Cox[1,2], Andrew Pekosz[1,2,6], and Sabra L. Klein[1,2*]

[1]W. Harry Feinstone Department of Molecular Microbiology and Immunology, Johns Hopkins University Bloomberg School of Public Health, Baltimore, MD, USA

[2]Department of Medicine, Division of Infectious Diseases, Johns Hopkins School of Medicine, Baltimore, MD, USA

[3]Office of Women's Health, U.S. Food and Drug Administration, Silver Spring, MD, USA

[4]Division of Urology, Obstetrics, and Gynecology; Office of Rare Diseases, Pediatrics, Urologic and Reproductive Medicine; Office of New Drugs; Center for Drug Evaluation and Research; U.S. Food and Drug Administration, Silver Spring, MD, USA

[5]Division of Viral Products, Center of Biologics Evaluation and Research, U.S. Food and Drug Administration, Silver Spring, MD, USA

[6]Department of Emergency Medicine, Johns Hopkins School of Medicine, Baltimore, MD, USA

[7]Department of Obstetrics, Gynecology and Reproductive Sciences, University of Maryland School of Medicine, Baltimore, MD, USA

[8]Department of Obstetrics and Gynecology, Johns Hopkins School of Medicine, Baltimore, MD, USA

*Address correspondence to Sabra L. Klein, (410)955-8898, sklein2@jhu.edu

Abstract

Pregnant individuals are at heightened risk for severe outcomes from many infectious diseases, including COVID-19. However, they were not included in the initial COVID-19 vaccine clinical trials and current rates of vaccine uptake among pregnant people remain below 15%. We defined the serological and cellular responses to COVID-19 mRNA booster vaccines (i.e., ancestral and BA.5) in pregnant and age-matched non-pregnant females to identify how pregnancy affects immunity against vaccine viruses in addition to novel variants. Blood was collected from participants prior to and 3-5 weeks post booster vaccine. Post-vaccination antibodies from pregnant participants were less cross-reactive to non-vaccine antigens, including XBB1.5 and JN.1, than antibodies from non-pregnant females. Antibodies from non-pregnant females showed strong correlations between IgG1 and FcR binding and greater IgG1:IgG3 ratios and live virus neutralization against all variants. In contrast, antibodies from pregnant participants had lower IgG1:IgG3 ratios and neutralization and greater antibody-dependent NK cell cytokine production and neutrophil phagocytosis, particularly against variants. CD4+ T cells from pregnant patients exhibited reduced polyfunctionality, with IFNγ+ monofunctional dominance. In contrast, among non-pregnant participants, CD4+ T cells displayed greater polyfunctionality, with more IL-21+ cells. Pregnancy may reduce the breadth, composition, and magnitude of humoral and cellular immunity, particularly in response to novel variants, highlighting the need for continued vaccination in this at-risk population.

46 **Introduction**

47 Pregnant individuals faced significant morbidity and mortality during the COVID-19
48 pandemic, with an elevated risk for severe outcomes [1-3]. From the onset of the pandemic
49 in early 2020 to December 2022, there were 24,203 cases of COVID-19 among pregnant
50 people in the United States with 2,043 fatalities [4]. This 8.4% mortality rate is significantly
51 higher than that of the general population (0.061%), reflecting the elevated risk for disease
52 outcomes in pregnancy. Pregnant individuals also are more likely to require hospitalization
53 and invasive ventilation from acute SARS-CoV-2 infection than non-pregnant people [3, 4].
54 Adverse pregnancy outcomes are an additional concern as SARS-CoV-2 infection has been
55 associated with preeclampsia, stillbirth, NICU admission, and preterm birth in people [1, 5,
56 6] and mouse models [7].

57 The Centers for Disease Control and Prevention (CDC) and the American College of
58 Obstetricians and Gynecologists (ACOG) recommend vaccination during pregnancy to
59 provide optimal protection against SARS-CoV-2 for both the mother and fetus [8]. Data
60 from November 2021 show vaccination rates among pregnant people (45.1%) were
61 significantly lower than that of non-pregnant people (64.9%) [9]. Vaccination rates among
62 pregnant people have since fallen precipitously, and remain lower than non-pregnant
63 people, with less than 15% of pregnant individuals vaccinated in the 2023-2024
64 vaccination season [10]. This decline in vaccine uptake is particularly concerning given that
65 other vaccines offered during pregnancy, such as influenza and Tdap, show higher coverage
66 rates (47.4% and 59.6%, respectively) [10, 11]. Despite proven safety of COVID-19 vaccines

67 during pregnancy [12], low vaccine uptake may be a result of greater vaccine hesitancy in
68 this population [13-15] (Parish et al., 2024b, submitted).

69 While vaccination is the best preventative strategy to reduce the severity of COVID-
70 19 outcomes [12, 16], existing evidence suggest pregnant individuals mount dampened
71 immune responses to vaccination, highlighting the need for deeper immunological
72 assessments [17]. Previous studies of COVID-19 vaccines in pregnant people have focused
73 on placental antibody transfer following vaccination during pregnancy, demonstrating the
74 benefits of maternal vaccination in protecting newborns and infants from severe infection
75 [18-20]. While several studies have aimed to compare the antibody landscape induced by
76 vaccination during pregnancy to those in non-pregnant people [21], to date, the effects of
77 pregnancy on cross-protection against circulating variants in addition to vaccine antigens
78 has remained unexplored.

79 Using systems serology, we can broadly and deeply characterize the antibody
80 landscape in response to COVID-19 vaccination. By employing this systematic and
81 comprehensive approach, we can gain insight to shape future vaccine development and
82 public health campaigns by understanding the protective immune response generated by
83 vaccination [22]. Combining functional assays and systems serology methods, we show
84 that the breadth and diversity of antibody generated by vaccination and polyfunctionality of
85 spike-specific memory CD4+ T cells are reduced during pregnancy, reinforcing the need for
86 vaccination, and boosting in pregnant individuals to ensure continued protection against
87 emerging variants.

88

89 **Methods**

90 ***Study Design***

91 Pregnant people were enrolled into mRNA vaccine studies at the Johns Hopkins Maternal &
92 Fetal Medicine Clinic (IRB 00246472) (n=7 pregnant) during the 2022-2023 vaccination
93 season. Pregnant participants were contacted at clinical visits or via phone to determine
94 interest and eligibility. Participants were eligible if they planned to receive an mRNA COVID
95 booster vaccine (Pfizer of Moderna) during weeks 32 through 36 of pregnancy, and consent
96 to maternal blood collection before and after receipt of the booster vaccine. Patients who
97 had already received an initial dose(s) of the vaccine were still eligible to enroll. Throughout
98 recruitment, 232 pregnant individuals were approached to participate in this study. Ninety-
99 one patients were initially interested while only 14 enrolled in the study. Of these, 7
100 completed the study. For non-pregnant female comparators, samples were obtained from
101 age-matched adult female healthcare workers who were recruited during the 2022-2023
102 influenza vaccine enrollment period by fliers, emails, and announcements about the
103 annual vaccination program and were able to self-enroll upon receipt of the influenza
104 vaccine at the Johns Hopkins East Baltimore hospital (IRB00288258) (n = 13 non-pregnant).
105 Demographic information is detailed in **Table 1**. Of the vaccinees enrolled, 13 age-matched
106 non-pregnant females received the COVID-19 booster vaccine during the same vaccination
107 season and had pre- and post-vaccination blood samples available. Plasma and peripheral
108 blood mononuclear cells were obtained prior to and one month after receipt of mRNA
109 booster vaccines from pregnant and non-pregnant patients. Plasma was used to assess
110 antigen-specific immunoglobulin isotype responses and live virus neutralizing antibody

111 responses, in addition to the crystallizable fragment (Fc) receptor affinity and non-
112 neutralizing antibody functions. Cryopreserved PBMCs were used for flow cytometry
113 analyses.

114 ***Cells and Viruses***

115 Vero-E6-TMPRSS2 cells were obtained from the cell repository of the National
116 Institute of Infectious Diseases, Japan and were grown in complete media consisting of
117 Dulbecco's modified eagle medium (DMEM) (Gibco, Thermo Fisher Scientific), containing
118 10% fetal bovine serum (FBS) (Gibco, Thermo Fisher Scientific), 1 mM glutamine
119 (Invitrogen, Thermo Fisher Scientific), 1 mM sodium pyruvate (Invitrogen, Thermo Fisher
120 Scientific), 100 U/mL penicillin (Invitrogen, Thermo Fisher Scientific), and 100 µg/mL
121 streptomycin (Invitrogen, Thermo Fisher Scientific). Cells were incubated at 37°C in a
122 humidified incubator with 5% CO2.

123 Ancestral (hCoV-19/USA/DC-HP00007/2020; B.1, GISAID EPI_ISL_434688), BA.5
124 (hCoV-19/USA/MD-HP32103-PIDCNSQVGY/2022, GISAID EPI_ISL_15013106), XBB.1.5
125 (hCoV-19/USA/MD-HP40900-PIDYSWHNUB/2022, GISAID EPI_ISL_16026423), and JN.1
126 (hCoV-19/USA/MD-HP49672-PIDDVSVURS/2023, GISAID EPI_ISL_18623285) variants of
127 SARS-CoV-2 were isolated from Vero-E6-TMPRSS2 cells plated in 24-well plates as
128 previously described [23]. The consensus sequence of the virus isolate did not differ from
129 the sequence derived from the clinical specimen. The infectious virus titer was determined
130 on Vero-TMPRSS2 cells using a 50% tissue culture infectious dose (TCID50) assay as
131 described [24].

132 ***Microneutralization assays***

133 Plasma neutralizing antibodies [25] were determined as described for SARS-CoV
134 and modified for SARS-CoV-2 as described [26]. Two- fold dilutions of plasma, starting at a
135 1:20 dilution, were made using incomplete media (IM) - Dulbecco's modified eagle medium
136 (DMEM) (Gibco, Thermo Fisher Scientific), containing 1 mM glutamine (Invitrogen, Thermo
137 Fisher Scientific), 1 mM sodium pyruvate (Invitrogen, Thermo Fisher Scientific), 100 U/mL
138 penicillin (Invitrogen, Thermo Fisher Scientific), and 100 µg/mL streptomycin (Invitrogen,
139 Thermo Fisher Scientific). Infectious virus was added to the plasma dilutions at a final
140 concentration of 1 × 10^3 TCID50/mL or 100 TCID50 per 100 µL. The plasma-virus solution
141 was incubated at room temperature for 1 hour, and 100 µL of each dilution was added to 1
142 well of a 96-well plate of VeroE6-TMPRSS2 cells in hextuplicate. The cells were incubated
143 for 6 hours at 37°C with 5% CO2. The inoculum was replaced with fresh IM, and the cells
144 were incubated at 37°C with 5% CO2 for 3-4 days until cytopathic effect (CPE) is evident in
145 the no serum controls. The cells were fixed by the addition of 100 µL of 4% formaldehyde
146 for at least 4 hours at room temperature, and then stained with naphthol blue-black
147 overnight. The nAb titer was calculated as the highest serum dilution that eliminated the
148 CPE in 50% of the wells (NT50) and the AUC was calculated [27, 28].

149 ***Antigen-bead coupling***

150 Antigen-specific isotyping and Fc receptor binding affinity were multiplexed using a
151 Luminex Intelliflex in a 384-well format. Antigens used in this panel are as follows:
152 ancestral spike (S) and nucleocapsid (N) protein, BA.5, XBB.1.5, and JN.1 spike proteins
153 were obtained through the National Cancer Institute Serological Sciences Networks
154 (SeroNet) for COVID-19 [29]. Each antigen was coupled to unique bead MagPlex bead

155 regions (Luminex). Briefly, beads were activated by activation solution consisting of
156 activation buffer (0.1M NaH2PO4; pH 6.2), 50mg/mL 1-ethyl-3-[3-dimethylaminopropyl]
157 carbodiimide (EDC), and 50mg/mL Sulfo-NHS (N-hydroxysulfosuccinimide). Activated
158 beads were coupled to 25ug of antigen in coupling buffer (0.05M MES; pH 5.0). Activated
159 coupled beads were blocked with blocking buffer (PBS 1X, 0.1%BSA, 0.02% Tween-20,
160 0.05% Sodium azide; pH 7.4), washed with washing buffer (PBS 1X, 0.05% Tween-20) and
161 stored at 4C in PBS.

162 ***Luminex serological assays***

163 Serum was diluted 1:25 and was incubated with bead solution (20uL of each bead
164 region in 20mL of Luminex Assay Buffer - PBS 1X, 0.1% BSA, 0.05% Tween). This protocol
165 was followed for isotyping (IgM, IgG [IgG1-4], and IgA [IgA1-2]) and binding to the following
166 Fc receptors (FcRs): FcγRIIA-R, FcγRIIA-H, FcγRIIb, FcγRIIIA-V, FcγRIIIA-F, FcγRIIIB, FcRn,
167 and FcαR (Duke Vaccine Institute – Protein Production facility). Following incubation,
168 plates were placed on a magnet and washed with Procartaplex Wash Buffer
169 (ThermoFisher). Each assay plate was then incubated with 45uL of secondary antibody
170 diluted in Luminex Assay Buffer. Isotypes were identified by PE-conjugated antibodies
171 (Southern Biotech) and FcR proteins were biotinylated using BirA biotin-ligation kit (Avidity)
172 at least one day prior and coupled to PE-Streptavidin (BioLegend). Following incubation
173 with secondary antibody, plates were placed on a magnet and washed. Beads were
174 resuspended in Procartaplex Wash Buffer before running on the Luminex Intelliflex.
175 Samples were run on FlexMap 3D Low with a DD range of 7000-1700. For each assay, the
176 MFI of secondary antibody-conjugated to PE, or FcR protein-conjugated to PE for each

177 bead region was measured on the Luminex Intelliflex to quantify antigen-specific
178 immunoglobulin isotypes and FcR responses in each sample at 0- and 28-days post
179 vaccination [30].

180 ***Antibody-dependent complement deposition (ADCD)***

181 Serum (1:15 dilution) was added to the MagPlex antigen coated beads. Plates were
182 incubated, placed on a magnet, and washed 3 times with 1% BSA. Lyophilized Low-Tox
183 Guinea Pig Complement (Cedarlane) was reconstituted in ice-cold dH2O and diluted 1:25
184 in Gelatin Veronal buffer with Mg^{2+} & Ca^{2+} (GVB++) (Boston Bio). Diluted complement
185 protein was added to each well followed by incubation at 37C. IgG goat anti-guinea pig C3
186 (MP Biomedicals) was diluted 1:500 in 0.1% BSA and added to each well. After incubation,
187 Donkey-anti goat IgG secondary antibody-PE (ThermoFisher) was diluted 1:200 in 0.1% BSA
188 and added to each well. Beads were resuspended in 0.1% BSA and run on the Luminex
189 Intelliflex.

190 ***Antibody-dependent NK cell cytotoxicity (ADNK)***

191 Natural killer (NK) cells were isolated from donor blood. Whole blood was spun
192 down with a Ficoll gradient to harvest PBMCs and NK cells isolated from PBMCs using the
193 MagniSort™ Human NK cell Enrichment Kit (ThermoFisher) with adjustment to a final
194 concentration of 1.5 x 10^6 cells/mL in R10 media, and IL-15 (1ng/mL, Abcam) was added
195 and incubated overnight. Plates were coated with 3mg/mL antigen (ancestral, BA.5,
196 XBB.1.5, and JN.1 spike proteins – SeroNet), blocked with 5% BSA, washed, and dried
197 before adding serum (1:100 dilution). Inhibitor cocktail (2.5 uL CD107a-PeCy5 (BD
198 Bioscience - BDB555802) + 0.5mL BFA (Millipore Sigma) + 1 uL Golgi Stop (BD Bioscience)

199 + 9mL R10 media) was added to each well, incubated, and surface staining cocktail (1uL
200 CD3-Pacific Blue (BD Bioscience - BDB558117) + 1mL CD56-PE-Cy7 (BD Bioscience -
201 BDB557747) + 1mL CD16-APC-Cy7 (BD Bioscience - BDB557758) + 7mL PBS) is added to a
202 V-bottom 96 well plate. NK cells were transferred to the V-bottom 96 well plate with pre-
203 added surface stain cocktail and incubated. Cells are spun down, supernatant removed,
204 and Perm A (ThermoFisher) was added to each well. Cells were washed and Intracellular
205 staining cocktail (1mL IFNγ-APC (BD Bioscience -) + 1mL MIP1-B-PE (BD Bioscience -
206 BDB550078) + 48mL Perm B (ThermoFisher) was added to each well. Plates were washed,
207 cells were resuspended in PBS and run on a Symphony A3 through the Bloomberg Flow
208 Cytometry and Immunology Core. Gating strategy as follows: NK cells- CD3-, CD16+,
209 CD56+ with reported cell populations including IFNγ+, CD107a+ and MIP1-B+ NK cells.

210 ***Antibody-dependent neutrophil phagocytosis (ADNP)***

211 Antigens (ancestral, BA.5, XBB.1.5, and JN.1 spike proteins – SeroNet) were
212 biotinylated with the BirA biotin-ligation kit (Avidity) and coupled to FluoSpheres™
213 NeutrAvidin™-Labeled Microspheres, 1.0 µm, yellow-green fluorescent (505/515)
214 (ThermoFisher). Antigen was combined with Neutravidin beads and incubated. Serum was
215 diluted 1:100 in PBS and incubated with antigen coated beads. During incubation, cells
216 were isolated from donor blood. Whole blood was collected into CPT tubes and spun at
217 1000rpm for 30min. Granulocytes were collected from below the density gradient. Cells
218 were suspended 1:10 in ACK Lysis buffer and incubated at RT for 5 min to lyse red blood
219 cells. Cells were washed and resuspended in 10mL of PBS. Plates were washed with PBS,
220 200mL of neutrophil solution (5 x 10^6 cells/plate) was added to each well, incubated,

221 spun at 500g for 5 min, and cells were resuspended in extracellular staining solution (0.5
222 mL APC CD66b (BioLegend - 305117) + 19.5mL PBS / well) and incubated for 15min
223 covered with foil at RT. After staining, plates were washed and resuspended in 4% PFA to fix
224 cells, washed and resuspended in PBS. Plates were run on the Attune NxT flow cytometer.
225 Gating on CD66b+ cells (neutrophils) followed by bead+ neutrophils, stained with APC.
226 Data are reported as a PhagoScore, calculated as (% bead positive neutrophils) *
227 (geometric MFI of each cell) [31].

228 ***Antibody-dependent cellular phagocytosis (ADCP)***

229 THP-1 cells, a human monocytic cell line, were plated 2.5 x 10^4 per well. Cells were
230 grown in suspension and diluted with warm R10 media. Following immune complex
231 formation, assay plates are washed with PBS and centrifuged at 2000g for 10min. The THP-
232 1 cells were added, and plates were incubated O/N at 37C. THP-1 cells were fixed, washed,
233 and resuspended in PBS. Plates are run on the Attune NxT flow cytometer. Gating included
234 bead+ single-cells stained with APC, representing THP-1 cells that have phagocytosed
235 bead. Data are reported as a PhagoScore, calculated as (% bead positive neutrophils) *
236 (geometric MFI of each cell) [32].

237 ***Ex vivo flow cytometry staining***

238 PBMCs were used to assess phenotype and function of immune cells. For broad
239 immune cell phenotyping (BIP), cells were stained for viability with Biolegend Live/Dead
240 Zombie NIR Fixable Viability Dye (423105) and BD Biosciences Fc Block™ (564219). Cell
241 surface staining was performed with surface antibody cocktail mix (**Supplementary**
242 **Methods Table 1A**). Cells were fixed and permeabilized with a 1X Fixation/Permeabilization

243 buffer from eBioscience FoxP3/Transcription Factor Staining Buffer Set. Intracellular
244 staining was performed with intracellular antibody cocktail mix (**Supplementary Methods**
245 **Table 1B**). Cells were resuspended in 1% paraformaldehyde and run on the 4-laser (16UV-
246 16V-15B-8R) Cytek Biosciences Aurora spectral flow cytometer. Data were exported for
247 further analysis in FlowJo for analysis (**Supplemental Figure 4**).

248 Intracellular cytokine flow cytometry staining was used to assess antigen-specific
249 cytokine production and T cell phenotypic and functional profiles. Cryopreserved PBMCs
250 were thawed, rested, and cultured overnight with 1 mg/mL peptide pools consisting of 315
251 peptides (15mers with 11 amino acid overlap) spanning the ancestral SARS-CoV-2 spike
252 protein (JPT Peptide Technologies, PM-WCPV-S-1) or a DMSO (unstimulated) control. After
253 overnight incubation, cells were washed and stained for flow cytometry as described for
254 BIP with the following variation: staining for viability was with Invitrogen Live/Dead Fixable
255 Blue Dead Cell Stain (L34962) and with T-cell panel surface and intracellular cytokine
256 antibody cocktails (**Supplementary Methods Table 2A-B**). For ICS, data were processed
257 using biexponential transformation and exported for further analysis in FlowJo to assess
258 cytokine-producing, antigen-specific T cells (**Supplemental Figure 5**). Polyfunctionality of
259 these T cells was analyzed with Pestle v2.0 and SPICE 6 v6.1.

260 ***Statistical analyses***

261 GraphPad Prism v10.1 was used to perform univariate analyses with details about
262 statistical tests used for each dataset in figure legends. Spearman correlations of systems
263 serology measures were visualized in heatmaps generated using R v4.2.3 and version
264 1.0.12 of the package "pheatmap" (https://cran.r-project.org/web/packages/pheatmap)

265 [33]. For ADNP and ADNK assays, data were averaged across two healthy donors. Flow FCS
266 files were analyzed using FlowJo v10 (10.8.1) software. Gating strategy for BIP and ICS can
267 be found in **Supplementary Figures 1** and **2**, respectively. ICS and BIP data were exported
268 from Pestle v2.0 and SPICE 6 v6.1 for further statistical analyses detailed in figure legends.
269

270 **Results**

271 ***Pregnancy alters IgG subtype dominance in response to novel variants***

272 Because SARS-CoV-2 nucleocapsid (N) antibodies are not generated by mRNA
273 vaccines targeted to S protein, this can be used as a proxy for SARS-CoV-2 infection [34],
274 with recognized limitations [25]. There was no increase in either anti-N IgG **(Figure 1A)** or in
275 any subclass of IgG **(Supplemental Figure 1A)** in any participants, suggesting that no one
276 was infected with SARS-CoV-2 during their study enrollment window. However, all
277 participants had detectable anti-N IgG levels highlighting prior exposure to SARS-CoV-2 in
278 our cohort. Luminex bead assays were used to comprehensively characterize the antibody
279 response generated by vaccination against SARS-CoV-2 vaccine antigens (ancestral and
280 BA.5 S) and other variants (XBB.1.5 and JN.1 S). COVID-19 boosters induced IgG in both
281 pregnant and non-pregnant females to vaccine and circulating variants **(Figure 1B)**. Prior to
282 vaccination, total IgG to ancestral S and BA.5 S was high in both cohorts as SARS-CoV-2
283 exposure through infection and prior vaccination is pervasive in the general population
284 [35]. However, there were distinct differences in the IgG subtype dominating this response.
285 There was IgG1 subtype dominance among non-pregnant, but not pregnant, females
286 **(Figure 1C-F).** While contributing to a small proportion of total IgG generated in response

287 to vaccination, pregnant individuals were more likely to induce anti-S IgG3 than non-
288 pregnant females **(Supplemental Figure 1 B-E).**

289 ***Pregnancy reduces the cross-neutralizing capacity of antibodies recognizing SARS-***
290 ***CoV-2 variants***

291 The ratio of IgG1:IgG3 has been shown to be predictive of SARS-CoV-2 neutralization
292 capacity [36]. Compared to non-pregnant females, pregnant individuals had reduced
293 IgG1:IgG3 ratios, particularly to circulating variants, demonstrating that the dominant IgG1
294 response in non-pregnant females may be indicative of broader cross-neutralization
295 **(Figure 2A-D).** This was reflected by reduced live virus neutralizing antibody [25] titers in
296 pregnant compared with non-pregnant individuals to variants. Both cohorts showed a rise
297 in neutralizing antibody titers to ancestral and BA.5 viruses after vaccination and were able
298 to effectively neutralize these viruses **(Figure 2E-F)**. Pregnant individuals, however, had
299 significantly lower nAb titers than non-pregnant females, with many pregnant individuals
300 failing to reach the limit of detection **(Figure 2G-H)**. In response to XBB.1.5, while
301 vaccination significantly increased nAb titers in both groups, these responses were
302 significantly higher in non-pregnant than pregnant females. Likewise, among non-pregnant
303 females, vaccination boosted nAb titers against JN.1; there was, however, no vaccine-
304 induced increase in nAb titers among pregnant individuals, with only 2/7 surpassing the
305 limit of detection. **(Figure 2G-H)**. These data suggest that there is reduced breadth and
306 cross-reactivity to variants after COVID-19 boosting among pregnant compared with non-
307 pregnant females.

308 ***Fc receptor affinity is not maintained in pregnant individuals against novel variants***

309 While neutralizing antibody titers are considered a correlate of protection for SARS-
310 CoV-2 infection [37], non-neutralizing functions also are important and may contribute to
311 robust protection from severe disease [38]. Data from mouse models suggest FcR binding
312 affinity and its associated effector functions are necessary for preventing severe COVID-19
313 disease [39]. To further understand protection provided by mRNA boosters in pregnant
314 individuals, we investigated FcR binding affinity. Antibody Fc binding affinity to FcγRIIA-R,
315 FcγRIIA-H, FcγRIIb, FcγRIIIA-V, FcγRIIIA-F, FcγRIIIB, FcRn, and FcαR was assessed by a
316 multiplexed Luminex bead assay. FcR binding affinity was similarly induced by vaccination
317 in response to ancestral and BA.5 vaccine antigens among both non-pregnant and
318 pregnant females **(Figure 3A-B).** While non-pregnant females saw similar increases in FcR
319 affinity to non-vaccine antigens following vaccination, vaccination did not induce changes
320 in FcR affinity in pregnant people, with no increase in affinity to 4/6 FcγRs in response to
321 XBB1.5 and 2/6 FcγRs in response to JN.1 (**Figure 3C-D**).

322 ***Non-neutralizing antibody functions and nAb are negatively correlated among***
323 ***pregnant individuals***

324 In order to understand how Fc binding affinity contributes to immunity generated by
325 COVID-19 vaccination, several non-neutralizing antibody functions were assessed. Non-
326 neutralizing functions aid in the clearance of infected cells through recruiting effector cells
327 [40]. Antibody dependent complement deposition (ADCD) was analyzed with a multiplexed
328 Luminex bead assay to measure antibody binding to complement protein C3 as a broad
329 indicator of the ability of serum antibody to induce activation of the complement cascade
330 [30]. ADCD was induced by vaccination in both cohorts in response to only XBB.1.5.

331 (**Figure 4A**). As ADCD to ancestral and BA.5 S was high in pre-vaccination samples, it is
332 likely that there were high preexisting immune responses through complement activation in
333 both cohorts.

334 In pregnancy, macrophage inflammatory protein (MIP)-1β+ NK cells are found at the
335 maternal-fetal interface and are important for successful implantation and placentation
336 [41]. In NK cells, MIP-1β acts as a chemoattractant in response to activation [42]. Antibody-
337 dependent NK cell cytotoxicity (ADNK) can be measured through MIP-1β production by NK
338 cells [43]. MIP-1β+ NK cells were uniquely elevated in pregnant people following
339 vaccination when compared to non-pregnant females (**Figure 4B**). In NK cells, interferon
340 gamma (IFNγ) acts as an antiviral cytokine to promote further accumulation, activation,
341 and cytotoxicity of NK cells [44]. As an additional readout of ADNK, NK cell IFNγ production
342 post-vaccination was elevated in pregnant individuals in response to BA.5 S, and in non-
343 pregnant females in response to JN.1 S **(Supplemental Figure 2A).** There were no changes
344 post-vaccination in NK cell degranulation, as marked by CD107a+ NK cells, among either
345 cohort **(Supplemental Figure 2B)**.

346 Antibody-dependent cellular phagocytosis (ADCP) and antibody-dependent
347 neutrophil phagocytosis (ADNP) assess the ability of antibody to induce macrophage and
348 neutrophil phagocytosis of antigen, respectively, and are reported as a PhagoScore [31],
349 representing both the function and number of beads phagocytosed. ADCP and ADNP
350 decreased following vaccination against vaccine and variant antigens (**Figure 4C-D**). This is
351 likely indicative of a shift towards neutralization and away from non-neutralizing cellular
352 functions, a phenomenon that has been documented in the context of repeat vaccination

353 and may be a result of immune imprinting mechanisms [45]. Correlation analyses revealed
354 significant negative correlations between nAb titers and ADNP PhagoScores among
355 pregnant participants only, further suggesting a shift away from neutralization, and towards
356 non-neutralizing neutrophil phagocytosis among pregnant people (**Figure 4E-H**). In non-
357 pregnant females, correlations were not significant, suggesting antibody responses marked
358 by both cellular non-neutralizing and neutralizing antibody function, indicative of a more
359 comprehensive and multi-pronged immune response generated by vaccination.

360 ***Altered correlations among IgG subclasses and antibody functional phenotypes in***
361 ***pregnant individuals***

362 Correlation matrices can be used to examine complex relationships between
363 antibody isotypes and effector functions assessed by systems serology [46]. These
364 analyses can highlight isotype dependence and may reveal differences in subclass
365 functionality [46]. Spearman correlation matrices were generated to assess correlations
366 between Ig isotypes and FcR affinity and antibody functional properties post-vaccination in
367 response to vaccine and variant viruses (**Figure 5**). Matrices were most different between
368 pregnant and non-pregnant people for variants, with fewer strong correlations in pregnant
369 than non-pregnant participants. Among non-pregnant people, IgG1 was positively and IgG3
370 was negatively correlated with FcR binding as well as neutralizing and non-neutralizing
371 antibody functions, particularly against variants. This trend was reversed in pregnant
372 participants, with positive trends with IgG3 and negative trends with IgG1. These data
373 further implicate the reduced IgG1:IgG3 ratio and isotype subclass switching as
374 functionally altering antibody-mediated immunity in pregnant people.

375 ***Decreased polyfunctional CD4⁺ T cells responses in pregnant people***

376 Because immunoglobulin subtype switching depends on CD4⁺ T cell help and
377 cytokine production [47], we hypothesized that differences in CD4⁺ T cell cytokine
378 production between pregnant and nonpregnant people might contribute to differences in
379 isotype switching and IgG subtypes. We assessed intracellular cytokine production by
380 CD4+ T cells in pregnant and non-pregnant participants in response to ancestral S peptide
381 pools [48, 49]. Intracellular cytokine staining of CD4+ T cells in response to ancestral S
382 peptide stimulation at post-vaccination timepoints demonstrated IFNγ+ monofunctional
383 dominance in pregnant participants, represented by an expansion of the dark purple slice
384 (**Figure 6A**). In CD4+ T cells, IFNγ production is known to modulate class switching in B
385 cells, particularly favoring IgG3 over IgG1 [50-52]. Conversely, non-pregnant female
386 participants demonstrated more broadly polyfunctional CD4+ T cell responses, defined as
387 producing two or more cytokines and highlighted by the arcs (**Figure 6B**). A greater
388 proportion of polyfunctional CD4+ T cells in the non-pregnant participants were IL-21+,
389 represented by the green arc (**Figure 6B**). IL-21 is a cytokine that induces B cells to
390 differentiate into antibody secreting cells [53] and has been linked to improved antibody
391 responses to vaccination [48, 54-56]. Polyfunctional CD4+ T cell responses can enhance
392 nAb titers and immunity following vaccination against multiple pathogens, including SARS-
393 CoV-2 [57-59].

394 ***Polymorphonuclear myeloid-derived suppressor cells are increased during pregnancy***

395 Polymorphonuclear myeloid-derived suppressor cells (PMN-MDSCs) have
396 previously been studied in the context of pregnancy, as they are required to maintain

397 maternal-fetal tolerance and are critical for fetal development [60, 61]. Their role, however,
398 has not been defined in the context of vaccination during pregnancy. There were no
399 detectable PMN-MDSCs in nonpregnant individuals, whereas the percentage in pregnant
400 individuals ranged from 0 to 1.5% of live PBMCs (**Supplemental Figure 3A**). The
401 percentage of low-density neutrophils also tended to be greater in pregnant participants
402 (**Supplemental Figure 3B**), but small sample sizes preclude deeper analysis. The
403 percentages of both PMN-MDSCs and neutrophils were negatively correlated with CD4+ T
404 cell cytokine production (**Supplemental Figure 3C**).
405

406 **Discussion**

407 Through broad characterization of the antibody landscape following COVID-19
408 vaccination, pregnancy was associated with reduced cross-protective antibody responses,
409 reflected in decreased IgG1:IgG3 ratios, nAb titers, and FcR binding affinity in pregnant
410 people. Previous studies have assessed the antibody profile generated by COVID-19
411 vaccination during pregnancy [18, 21, 62], with a focus on transplacental antibody transfer
412 and protection of babies and infants from severe disease. One study showed limited cross-
413 recognition in pregnant individuals to non-vaccine antigens after the first doses of
414 ancestral vaccines, with no comparisons to non-pregnant controls [18]. Our data illustrate
415 that pregnancy is associated with reduced isotype class switching and nAb responses to
416 variants as compared with non-pregnant controls. Continuing efforts to assess antibody
417 responses to updated vaccines remains critical to understanding cross-protection to
418 variants in circulation.

419 SARS-CoV-2 has continued to rapidly evolve and mutate into new variants to escape
420 adaptive immune responses [63]. In 2022, Omicron variants became dominant in
421 circulation, largely due to an ability to evade nAb generated by ancestral vaccines and
422 natural infections [64]. New variants with the ability to evade nAb continue to emerge and
423 dominate, with XBB.1.5. appearing in October 2022 and peaking in January of 2023, after
424 the inclusion of BA.5 in bivalent booster vaccines was established [65]. By the time XBB.1.5
425 monovalent boosters were accessible, a new variant, JN.1 caused 60% of global cases [65,
426 66]. This reflects a limitation of annual vaccine campaigns in which there is a mismatch
427 between dominate circulating strains and updated booster vaccines because variants
428 continue to emerge between annual vaccines strain updates. While mRNA technology has
429 increased the speed in which companies can adapt updated vaccines to emerging
430 variants, development of a new booster vaccine still takes several months [67]. Thus,
431 government officials and researchers must work collaboratively to select strains for
432 booster vaccines that will elicit the greatest breadth of immunity [67]. In our study, almost
433 all individuals were vaccinated against ancestral and BA.5 (bivalent boosters), while
434 XBB.1.5. was the dominant variant in circulation. Our data provide mechanistic evidence
435 underscoring the critical importance of staying up to date with vaccinations, as pregnant
436 individuals have limited cross-protective antibodies that could be critical to protect
437 pregnant individuals and their babies from severe disease caused by variant viruses.
438 With repeated exposure to antigen through natural infection and booster vaccines,
439 antibody responses to COVID-19 vaccines have evolved and correlates of protection have
440 changed. Total IgG and nAb titers are considered adequate correlates of protection against

441 COVID-19, similar to other acute respiratory infectious diseases [68]. Recent data have
442 suggested that to mount sufficient protection, antibodies against SARS-CoV-2 must
443 possess both neutralizing and non-neutralizing functions as correlates of protection [69].
444 As nAb titers wane and symptomatic cases rise, hospitalization rates among the general
445 population remain low [70]. This provides evidence that other antibody characteristics may
446 be important for protection from severe disease. Our data demonstrate that pregnant
447 participants had reduced FcR binding and nAb responses combined with elevated ADNK
448 and ADNP, especially to non-vaccine antigens. These data might suggest that the shift from
449 neutralizing to non-neutralizing antibody responses against emerging variants could reduce
450 protection in pregnant individuals.

451 Our data suggest that reduced class switching and T cell polyfunctionality may
452 contribute to limited cross-reactivity of antibodies during pregnancy. There is trend for
453 PMN-MDSCs in PBMCs to be more frequent among pregnant than non-pregnant, which
454 might contribute to suppressed CD4+ T cell cytokine production and proliferation [36].
455 CD4+ T cells are critical for generation of high affinity, class switched antibodies and
456 contribute to vaccine-induced protection against COVID-19 [71]. Our data suggest that
457 reduced T-cell polyfunctionality during pregnancy may limit protection conferred to novel
458 variants. IL-21+ CD4+ T cells have been shown previously to be correlated with enhanced
459 vaccine responses, including COVID-19 vaccine responses [55]. Pregnant participants
460 showed reduced expansion of IL-21+ CD4+ T-cells, potentially contributing to reduced
461 class switching and the generation of nAb responses in pregnant people [48, 54-56].
462 Additionally, expansion of IFNγ+ monofunctional CD4+ T cells may further contribute to

463 reduced IgG1:IgG3 ratios among pregnant people as these cells promote IgG3 bias in B
464 cells [50-52].

465 The small sample size is a limitation of this study and was associated with challenges
466 recruiting pregnant participants. Previous studies have shown the impact of trimester on
467 immune responses generated by COVID-19 vaccination [12, 72]. In the present study,
468 sample size limited our ability to assess trimester differences, with 6/7 pregnant females
469 enrolled in our study being vaccinated in the second trimester of pregnancy. While 232
470 pregnant people were approached during the study enrollment window, only 7 completed
471 the study. This likely reflects the limited COVID-19 vaccine uptake among pregnant people,
472 which we show is caused by numerous factors across the care continuum that contribute
473 to COVID-19 vaccine hesitancy in this population (Parish et al. 2024b, submitted).
474 Identification of points of public health intervention to effectively increase vaccine uptake
475 among pregnant people is needed.

476 There are many factors contributing to COVID-19 vaccine hesitancy; lack of confidence
477 in vaccine safety, however, is a large contributor [13], especially with pregnant people being
478 excluded from early COVID-19 vaccine trials [73]. Continued research and public health
479 efforts to disseminate information on the safety and necessity of updated COVID-19
480 vaccination during pregnancy are needed to address gaps in understanding and to increase
481 vaccine uptake. By highlighting the lack of cross-protective antibody generated during
482 pregnancy, our data emphasize the continued need for updated vaccination among this at-
483 risk population [73].

Acknowledgements. We thank the clinical coordinators and vaccinees for making this study possible. We are especially grateful to Kimberly Jones-Beatty and Michelle Ufua for their assistance with recruitment. Thank you to Galit Alter, Ryan McNamara, and Taras Chicz for graciously training lab members and sharing protocols to develop systems serology methods. We thank Prakash Srinivasan for the use of the Attune Nxt flow cytometer.

Funding. FDA CERSI U01FD005942 (SLK), NIH NIAID 75N93021C00045 (AP, RR), NIH NCI U54 CA260492 (SLK, ALC).

Data Availability

All anonymized data that support the findings of this study and source data for the figures will be available through the NIH/NCI Serological Sciences Network for COVID-19 (SeroNet) data repository, accessible via ImmPort (https://www.immport.org). All other data are available from the corresponding author upon reasonable request.

Author Contributions

SLK, IB, AP, and ALC conceptualized the experimental design and group comparisons for this study. MAP, H-SP, JSL, LStC, PS, IB, JS, KF, RR, and ALC identified, acquired, stored, and distributed patient samples and clinical and demographic data for analyses. MAP, H-SP, PC, AW and JSL developed and validated serological assays. MAP, JS, LG and H-SP processed samples and completed technical assays. MAP, KR, and AY conducted

statistical analyses. MAP, LG, KR, ALC, and SLK developed all tables and figures. MAP, ALC, SLK wrote the initial draft of the manuscript. All authors provided substantive edits and approved the final draft of the manuscript.

References

1. Engjom, H.M., et al., *Perinatal outcomes after admission with COVID-19 in pregnancy: a UK national cohort study.* Nature Communications, 2024. **15**(1): p. 3234.
2. Brioschi Dos Santos, A.P., et al., *The impact of COVID-19 on maternal death and fetal death, a cohort study in Brazil.* PLoS One, 2023. **18**(8): p. e0290343.
3. St Clair, L.A., et al., *Reduced control of SARS-CoV-2 infection associates with lower mucosal antibody responses in pregnancy.* mSphere, 2024. **9**(3): p. e0081223.
4. Strid, P., et al., *Coronavirus Disease 2019 (COVID-19) Severity Among Women of Reproductive Age With Symptomatic Laboratory-Confirmed Severe Acute Respiratory Syndrome Coronavirus 2 (SARS-CoV-2) Infection by Pregnancy Status-United States, 1 January 2020-25 December 2021*. Clin Infect Dis, 2022. **75**(Suppl 2): p. S317-s325.
5. Wei, S.Q., et al., *The impact of COVID-19 on pregnancy outcomes: a systematic review and meta-analysis.* Cmaj, 2021. **193**(16): p. E540-e548.
6. Sessa, R., et al., *SARS-CoV-2 Infection in Pregnancy: Clues and Proof of Adverse Outcomes*. Int J Environ Res Public Health, 2023. **20**(3).
7. Creisher, P.S., et al., *Adverse outcomes in SARS-CoV-2-infected pregnant mice are gestational age-dependent and resolve with antiviral treatment.* J Clin Invest, 2023. **133**(20).
8. Ciapponi, A., et al., *Safety of COVID-19 vaccines during pregnancy: A systematic review and meta-analysis.* Vaccine, 2023. **41**(25): p. 3688-3700.
9. Razzaghi, H., et al., *COVID-19 vaccination coverage and intent among women aged 18-49 years by pregnancy status, United States, April-November 2021*. Vaccine, 2022. **40**(32): p. 4554-4563.
10. Katherine E. Kahn, E.G., Hilda Razzaghi, Tara C. Jatlaoui, Tami H. Skoff, Sascha R. Ellington, Carla L. Black, *Flu, Tdap, and COVID-19 Vaccination Coverage Among Pregnant Women – United States, April 2024*. 2024.
11. Razzaghi H, K.K., Calhoun K, et al., *Influenza, Tdap, and COVID-19 Vaccination Coverage and Hesitancy Among Pregnant Women — United States, April 2023*. MMWR Morb Mortal Wkly Rep, 2023.
12. Norman, M., et al., *Neonatal Outcomes After COVID-19 Vaccination in Pregnancy.* Jama, 2024. **331**(5): p. 396-407.
13. Casubhoy, I., et al., *A scoping review of global COVID-19 vaccine hesitancy among pregnant persons*. npj Vaccines, 2024. **9**(1): p. 131.

14. Oliver, J., et al., *Drivers of COVID-19 vaccine hesitancy among women of childbearing age in Victoria, Australia: A descriptive qualitative study*. Vaccine: X, 2022. **12**: p. 100240.
15. Hsu, A.L., et al., *Sources of Vaccine Hesitancy: Pregnancy, Infertility, Minority Concerns, and General Skepticism*. Open Forum Infectious Diseases, 2021. **9**(3).
16. Chavan, M., et al., *COVID-19 Vaccination in Pregnancy: The Benefits Outweigh the Risks*. J Obstet Gynaecol Can, 2021. **43**(7): p. 814-816.
17. Kay, A.W. and C.A. Blish, *Immunogenicity and Clinical Efficacy of Influenza Vaccination in Pregnancy*. Front Immunol, 2015. **6**: p. 289.
18. Lopez, P.A., et al., *Placental transfer dynamics and durability of maternal COVID-19 vaccine-induced antibodies in infants*. iScience, 2024. **27**(3): p. 109273.
19. Munoz, F.M., et al., *COVID-19 booster vaccination during pregnancy enhances maternal binding and neutralizing antibody responses and transplacental antibody transfer to the newborn*. Vaccine, 2023. **41**(36): p. 5296-5303.
20. Cassidy, A.G., et al., *Assessment of Adverse Reactions, Antibody Patterns, and 12-month Outcomes in the Mother-Infant Dyad After COVID-19 mRNA Vaccination in Pregnancy*. JAMA Netw Open, 2023. **6**(7): p. e2323405.
21. Atyeo, C., et al., *COVID-19 mRNA vaccines drive differential antibody Fc-functional profiles in pregnant, lactating, and nonpregnant women*. Sci Transl Med, 2021. **13**(617): p. eabi8631.
22. Ackerman, M.E., D.H. Barouch, and G. Alter, *Systems serology for evaluation of HIV vaccine trials*. Immunol Rev, 2017. **275**(1): p. 262-270.
23. Fall, A., et al., *The displacement of the SARS-CoV-2 variant Delta with Omicron: An investigation of hospital admissions and upper respiratory viral loads*. EBioMedicine, 2022. **79**: p. 104008.
24. Dhakal, S., et al., *Sex Differences in Lung Imaging and SARS-CoV-2 Antibody Responses in a COVID-19 Golden Syrian Hamster Model*. mBio, 2021. **12**(4): p. e0097421.
25. Dhakal, S., et al., *Reconsideration of Antinucleocapsid IgG Antibody as a Marker of SARS-CoV-2 Infection Postvaccination for Mild COVID-19 Patients*. Open Forum Infect Dis, 2023. **10**(1): p. ofac677.
26. Lee, J.M., et al., *Three doses of COVID-19 mRNA vaccine induce class-switched antibody responses in inflammatory arthritis patients on immunomodulatory therapies*. Front Immunol, 2023. **14**: p. 1266370.
27. Li, M., et al., *Convalescent plasma with a high level of virus-specific antibody effectively neutralizes SARS-CoV-2 variants of concern*. Blood Adv, 2022. **6**(12): p. 3678-3683.
28. Klein, S.L., et al., *Sex, age, and hospitalization drive antibody responses in a COVID-19 convalescent plasma donor population*. J Clin Invest, 2020. **130**(11): p. 6141-6150.
29. Karger, A.B., et al., *The Serological Sciences Network (SeroNet) for COVID-19: Depth and Breadth of Serology Assays and Plans for Assay Harmonization*. mSphere, 2022. **7**(4): p. e0019322.

589 30. Chung, A.W., et al., *Dissecting Polyclonal Vaccine-Induced Humoral Immunity*
590 *against HIV Using Systems Serology.* Cell, 2015. **163**(4): p. 988-98.
591 31. Karsten, C.B., et al., *A versatile high-throughput assay to characterize antibody-*
592 *mediated neutrophil phagocytosis.* J Immunol Methods, 2019. **471**: p. 46-56.
593 32. Loos, C., et al., *Systems serology-based comparison of antibody effector functions*
594 *induced by adjuvanted vaccines to guide vaccine design*. npj Vaccines, 2023. **8**(1): p.
595 34.
596 33. Kolde, R., *Pretty Heatmaps*. 2018. p. Implementation of heatmaps that offers more
597 control over dimensions and appearance.
598 34. Gaeta, A., et al., *Anti-N SARS-CoV-2 assays for evaluation of natural viral infection.* J
599 Immunol Methods, 2023. **518**: p. 113486.
600 35. Swadźba, J., et al., *High Concentration of Anti-SARS-CoV-2 Antibodies 2 Years after*
601 *COVID-19 Vaccination Stems Not Only from Boosters but Also from Widespread,*
602 *Often Unrecognized, Contact with the Virus.* Vaccines (Basel), 2024. **12**(5).
603 36. Chen, W., et al., *The kinetics of IgG subclasses and contributions to neutralizing*
604 *activity against SARS-CoV-2 wild-type strain and variants in healthy adults*
605 *immunized with inactivated vaccine.* Immunology, 2022. **167**(2): p. 221-232.
606 37. Sun, K., et al., *SARS-CoV-2 correlates of protection from infection against variants of*
607 *concern.* Nature Medicine, 2024. **30**(10): p. 2805-2812.
608 38. Izadi, A. and P. Nordenfelt, *Protective non-neutralizing SARS-CoV-2 monoclonal*
609 *antibodies.* Trends Immunol, 2024. **45**(8): p. 609-624.
610 39. Mackin, S.R., et al., *Fc-γR-dependent antibody effector functions are required for*
611 *vaccine-mediated protection against antigen-shifted variants of SARS-CoV-2.* Nat
612 Microbiol, 2023. **8**(4): p. 569-580.
613 40. Chandler, T.L., et al., *Protective mechanisms of nonneutralizing antiviral antibodies.*
614 PLoS Pathog, 2023. **19**(10): p. e1011670.
615 41. Du, M.R., S.C. Wang, and D.J. Li, *The integrative roles of chemokines at the*
616 *maternal-fetal interface in early pregnancy.* Cell Mol Immunol, 2014. **11**(5): p. 438-
617 48.
618 42. Bluman, E.M., et al., *Human natural killer cells produce abundant macrophage*
619 *inflammatory protein-1 alpha in response to monocyte-derived cytokines.* J Clin
620 Invest, 1996. **97**(12): p. 2722-7.
621 43. Boudreau, C.M., et al., *Antibody-mediated NK cell activation as a correlate of*
622 *immunity against influenza infection*. Nature Communications, 2023. **14**(1): p. 5170.
623 44. Lin, Q., et al., *IFN-γ-dependent NK cell activation is essential to metastasis*
624 *suppression by engineered Salmonella*. Nature Communications, 2021. **12**(1): p.
625 2537.
626 45. Tortorici, M.A., et al., *Persistent immune imprinting occurs after vaccination with the*
627 *COVID-19 XBB.1.5 mRNA booster in humans.* Immunity, 2024. **57**(4): p. 904-911.e4.
628 46. Atyeo, C., et al., *Distinct Early Serological Signatures Track with SARS-CoV-2*
629 *Survival.* Immunity, 2020. **53**(3): p. 524-532.e4.
630 47. Sha, Z. and R.W. Compans, *Induction of CD4(+) T-cell-independent immunoglobulin*
631 *responses by inactivated influenza virus.* J Virol, 2000. **74**(11): p. 4999-5005.

632 48. Thompson, E.A., et al., *Heterologous versus homologous boosting elicits*
633 *qualitatively distinct, BA.5-cross-reactive T cells in transplant recipients*. JCI Insight,
634 2023. **8**(10).
635 49. Roznik, K., et al., *COVID-19 vaccination induces distinct T-cell responses in*
636 *pediatric solid organ transplant recipients and immunocompetent children*. NPJ
637 Vaccines, 2024. **9**(1): p. 73.
638 50. Peng, S.L., S.J. Szabo, and L.H. Glimcher, *T-bet regulates IgG class switching and*
639 *pathogenic autoantibody production*. Proc Natl Acad Sci U S A, 2002. **99**(8): p. 5545-
640 50.
641 51. Alspach, E., D.M. Lussier, and R.D. Schreiber, *Interferon γ and Its Important Roles in*
642 *Promoting and Inhibiting Spontaneous and Therapeutic Cancer Immunity*. Cold
643 Spring Harb Perspect Biol, 2019. **11**(3).
644 52. Mohr, E., et al., *IFN-{gamma} produced by CD8 T cells induces T-bet-dependent and*
645 *-independent class switching in B cells in responses to alum-precipitated protein*
646 *vaccine*. Proc Natl Acad Sci U S A, 2010. **107**(40): p. 17292-7.
647 53. Wang, S., et al., *IL-21 drives expansion and plasma cell differentiation of*
648 *autoreactive CD11chiT-bet+ B cells in SLE*. Nature Communications, 2018. **9**(1): p.
649 1758.
650 54. Pallikkuth, S., et al., *Upregulation of IL-21 receptor on B cells and IL-21 secretion*
651 *distinguishes novel 2009 H1N1 vaccine responders from nonresponders among*
652 *HIV-infected persons on combination antiretroviral therapy*. J Immunol, 2011.
653 **186**(11): p. 6173-81.
654 55. Malahe, S.R.K., et al., *The role of interleukin-21 in COVID-19 vaccine-induced B cell-*
655 *mediated immune responses in patients with kidney disease and kidney transplant*
656 *recipients*. Am J Transplant, 2023. **23**(9): p. 1411-1424.
657 56. Fan, W., Y. Wan, and Q. Li, *Interleukin-21 enhances the antibody avidity elicited by*
658 *DNA prime and MVA boost vaccine*. Cytokine, 2020. **125**: p. 154814.
659 57. Darrah, P.A., et al., *Multifunctional TH1 cells define a correlate of vaccine-mediated*
660 *protection against Leishmania major*. Nat Med, 2007. **13**(7): p. 843-50.
661 58. Rakshit, S., et al., *Polyfunctional CD4 T-cells correlating with neutralising antibody is*
662 *a hallmark of COVISHIELDTM and COVAXIN® induced immunity in COVID-19*
663 *exposed Indians*. npj Vaccines, 2023. **8**(1): p. 134.
664 59. Li, L., et al., *In-depth analysis of SARS-CoV-2-specific T cells reveals diverse*
665 *differentiation hierarchies in vaccinated individuals*. JCI Insight, 2022. **7**(7).
666 60. Shi, M., et al., *Continuous activation of polymorphonuclear myeloid-derived*
667 *suppressor cells during pregnancy is critical for fetal development*. Cellular &
668 Molecular Immunology, 2021. **18**(7): p. 1692-1707.
669 61. Li, C., et al., *Upregulated TRAIL and Reduced DcR2 Mediate Apoptosis of Decidual*
670 *PMN-MDSC in Unexplained Recurrent Pregnancy Loss*. Frontiers in Immunology,
671 2020. **11**.
672 62. Atyeo, C.G., et al., *Maternal immune response and placental antibody transfer after*
673 *COVID-19 vaccination across trimester and platforms*. Nature Communications,
674 2022. **13**(1): p. 3571.

63. Markov, P.V., et al., *The evolution of SARS-CoV-2*. Nature Reviews Microbiology, 2023. **21**(6): p. 361-379.
64. Chi, W.Y., et al., *COVID-19 vaccine update: vaccine effectiveness, SARS-CoV-2 variants, boosters, adverse effects, and immune correlates of protection*. J Biomed Sci, 2022. **29**(1): p. 82.
65. Huiberts, A.J., et al., *Effectiveness of Omicron XBB.1.5 vaccine against infection with SARS-CoV-2 Omicron XBB and JN.1 variants, prospective cohort study, the Netherlands, October 2023 to January 2024*. Euro Surveill, 2024. **29**(10).
66. Rubin, R., *As COVID-19 Cases Surge, Here's What to Know About JN.1, the Latest SARS-CoV-2 "Variant of Interest"*. Jama, 2024. **331**(5): p. 382-383.
67. Monto, A.S., A.S. Lauring, and E.T. Martin, *SARS-CoV-2 Vaccine Strain Selection: Guidance From Influenza*. J Infect Dis, 2022. **227**(1): p. 4-8.
68. Regev-Yochay, G., et al., *Correlates of protection against COVID-19 infection and intensity of symptomatic disease in vaccinated individuals exposed to SARS-CoV-2 in households in Israel (ICoFS): a prospective cohort study*. The Lancet Microbe, 2023. **4**(5): p. e309-e318.
69. Goldblatt, D., et al., *Correlates of protection against SARS-CoV-2 infection and COVID-19 disease*. Immunol Rev, 2022. **310**(1): p. 6-26.
70. Mahrokhian, S.H., et al., *COVID-19 vaccines: Immune correlates and clinical outcomes*. Hum Vaccin Immunother, 2024. **20**(1): p. 2324549.
71. Kent, S.J., et al., *Disentangling the relative importance of T cell responses in COVID-19: leading actors or supporting cast?* Nature Reviews Immunology, 2022. **22**(6): p. 387-397.
72. Yang, Y.J., et al., *Association of Gestational Age at Coronavirus Disease 2019 (COVID-19) Vaccination, History of Severe Acute Respiratory Syndrome Coronavirus 2 (SARS-CoV-2) Infection, and a Vaccine Booster Dose With Maternal and Umbilical Cord Antibody Levels at Delivery*. Obstetrics & Gynecology, 2022. **139**(3): p. 373-380.
73. Klein, S.L., P.S. Creisher, and I. Burd, *COVID-19 vaccine testing in pregnant females is necessary*. J Clin Invest, 2021. **131**(5).

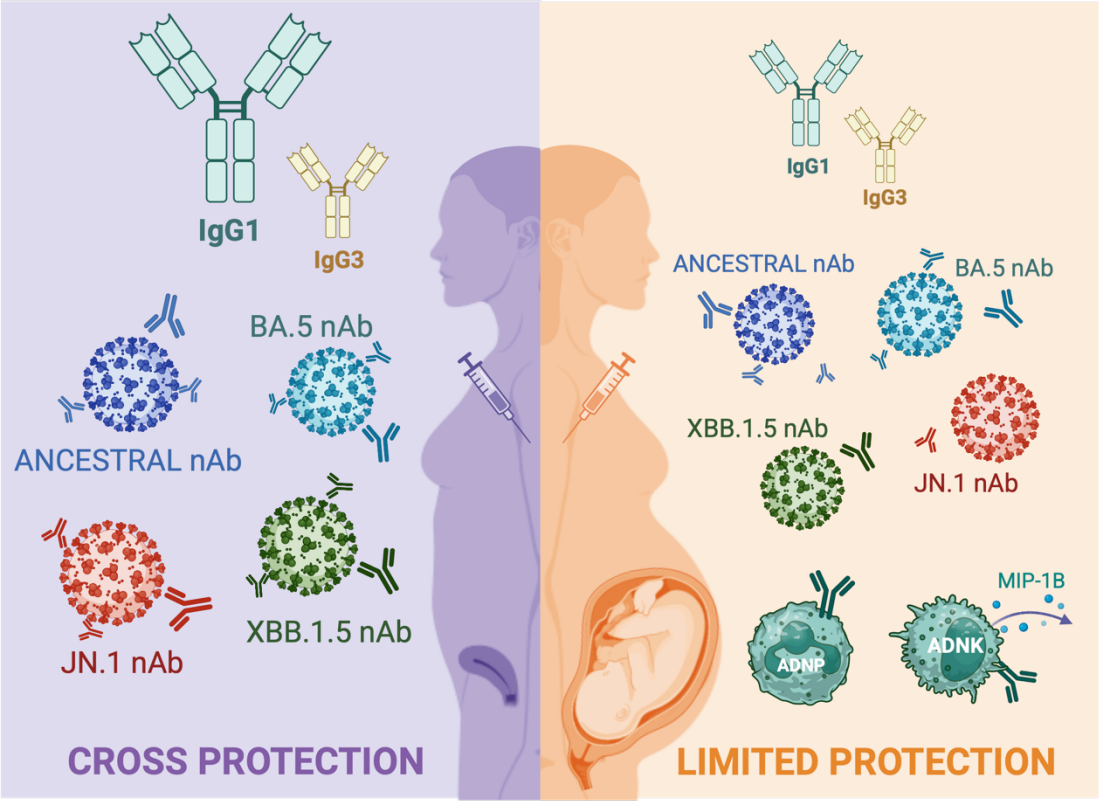

Graphical abstract

Table 1: Study Demographics

	Non-Pregnant n = 13	Pregnant n = 7	P-Value
Demographics	Mean ± SD	Mean ± SD	
Age	33.1 ± 6.1	32.9 ±3.2	0.93064
Vaccine Type			
Monovalent Booster	0 0%	2 28.5%	
Bivalent Booster	10 100%	5 71.5%	
Average Gestational Age (weeks)	-	22.4 ± 11.78	
	N %	**N %**	
Race			
White	8 61.5%	7 100%	
Black	2 15.4%	0 0%	
Asian	3 23.1%	0 0%	
Gestational Age (At Vaccination)	-	1st Trimester (n = 0) 0% 2nd Trimester (n = 6) 85.8% 3rd Trimester (n = 1) 14.2%	

Table 1.

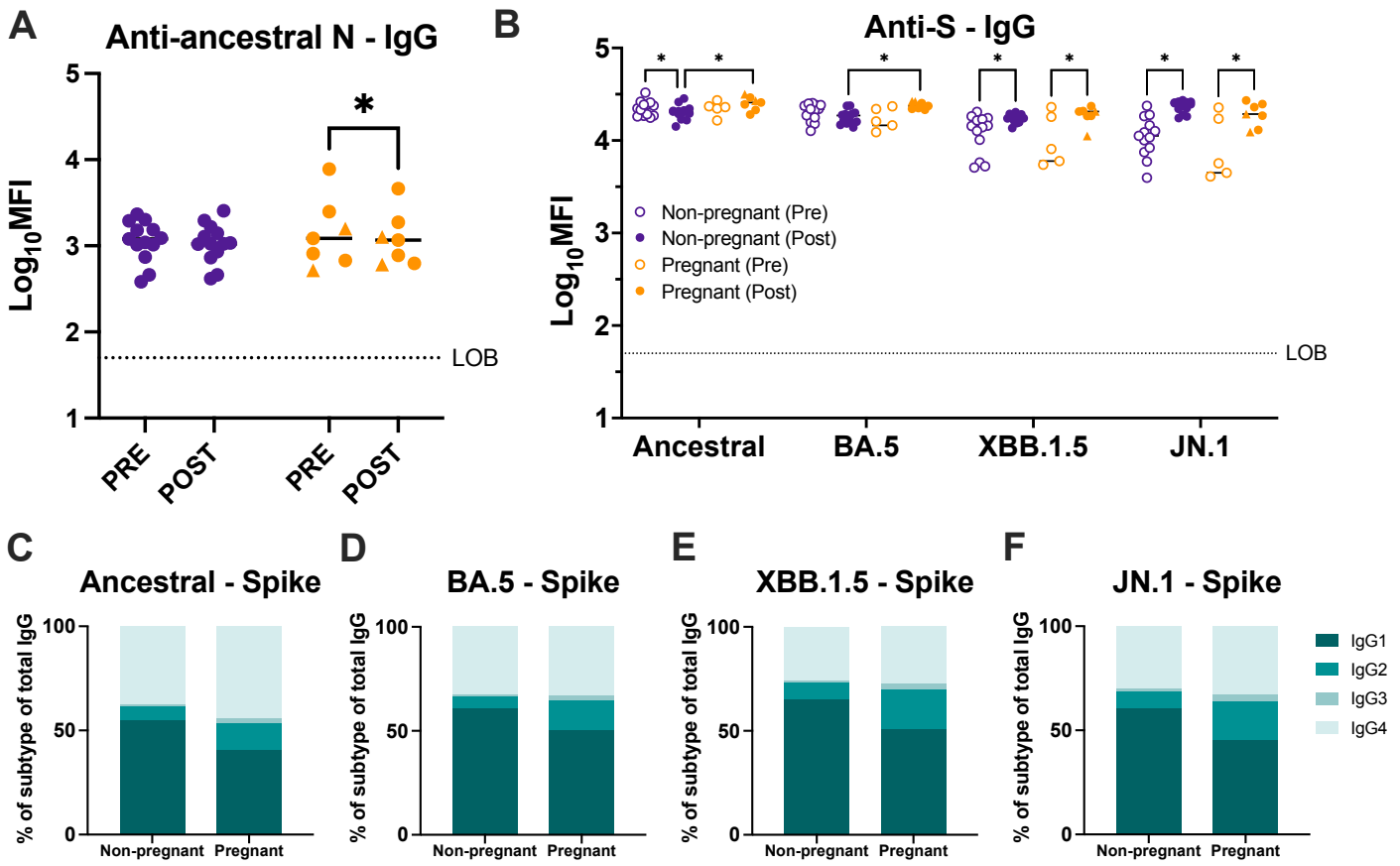

Figure 1. Vaccination differently induces IgG subtype responses during pregnancy. IgG antibody responses in serum pre and 3-5 weeks post-vaccination were measured by systems serology and reported as $\log_{10}$ mean fluorescence intensity (MFI). Pregnant individuals (n=7) are shown in orange and non-pregnant females (n=13) in purple. Triangles highlight individuals who received monovalent boosters and circles represent bivalent booster recipients. **(A)** Total IgG to ancestral nucleocapsid (N) protein**. (B)** Total IgG separated by SARS-CoV-2 vaccine (ancestral and BA.5) and variant (XBB1.5 and JN.1) spike (S) antigen and pregnancy status. **(C-F)** Relative abundance of IgG subtypes in pregnant and non-pregnant people as stacked bar plots representing each isotype as a percentage of Total IgG by **(C)** ancestral S, **(D)** BA.5 S, **(E)** XBB.1.5 S, and **(F)** JN.1 S. Data were analyzed by **(A)** repeated measures two-way ANOVA **(B-F)** linear mixed effects regression analysis with Bonferroni post-hoc. Asterisks indicate $p < 0.05$. Stippled line indicates limit of background (LOB) defined as the $\log_{10}$MFI of a defined negative control.

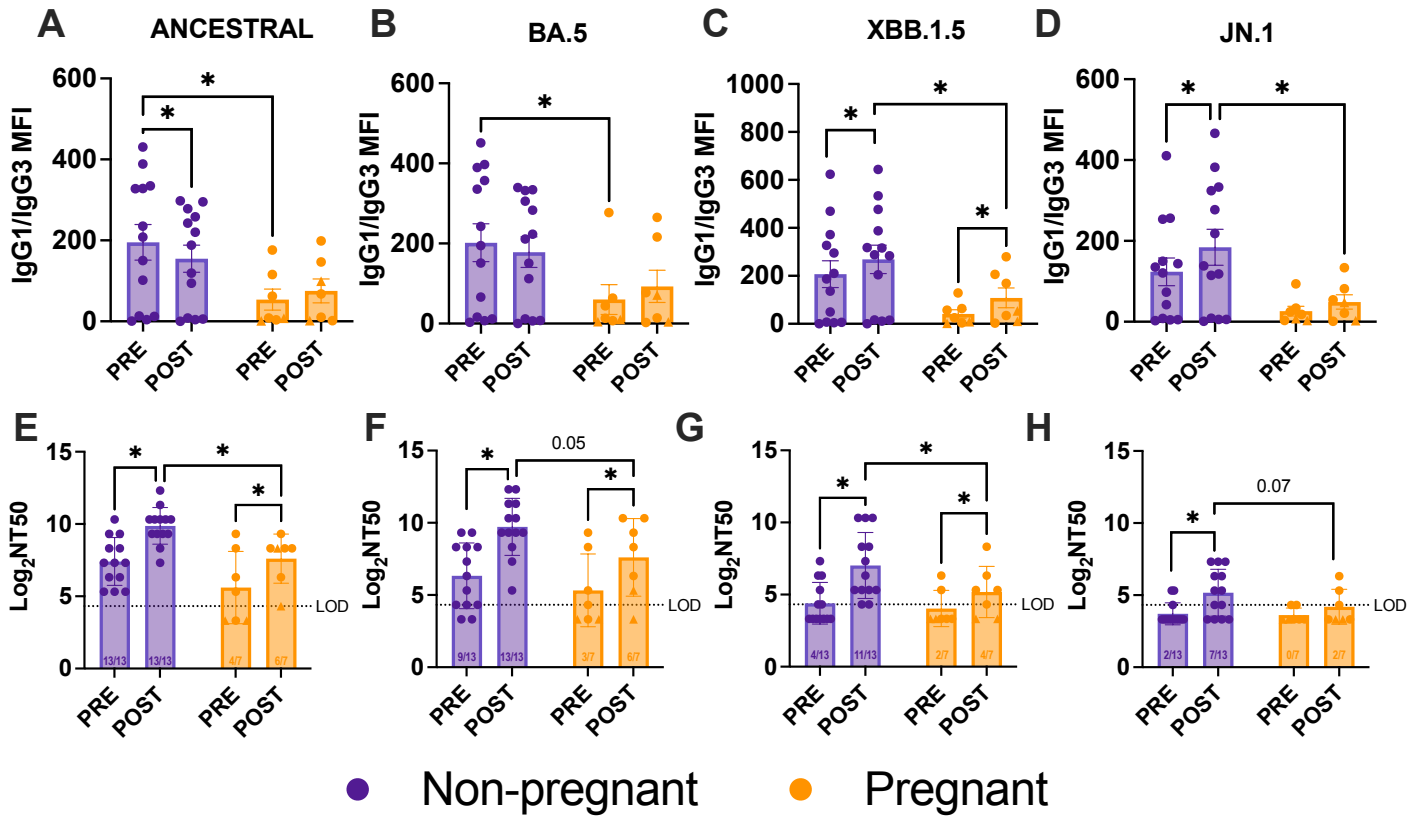

Figure 2. Pregnancy alters cross-neutralization of variants of concern. IgG antibody responses in serum pre and 3-5 weeks post-vaccination were measured by systems serology and reported as mean fluorescence intensity (MFI). Pregnant individuals (n=7) are shown in orange and non-pregnant females (n=13) in purple. Triangles highlight individuals who received monovalent boosters and circles represent bivalent booster recipients. **(A-E)** Ratio of IgG1:IgG3 antibodies specific to **(A)** ancestral spike (S), **(B)** BA.5 S, **(C)** XBB.1.5 S, and **(D)** JN.1 S. Neutralizing antibody (nAb) titers reported as Log_2 NT50 against live **(E)** ancestral, **(F)** BA.5, **(G)** XBB.1.5, and **(H)** JN.1 viruses. Ratios indicate number of individuals above the limit of detection (LOD) indicated by the stippled line. Data were analyzed by repeated measures two-way ANOVA with Bonferroni post-hoc. Asterisks indicate $p < 0.05$.

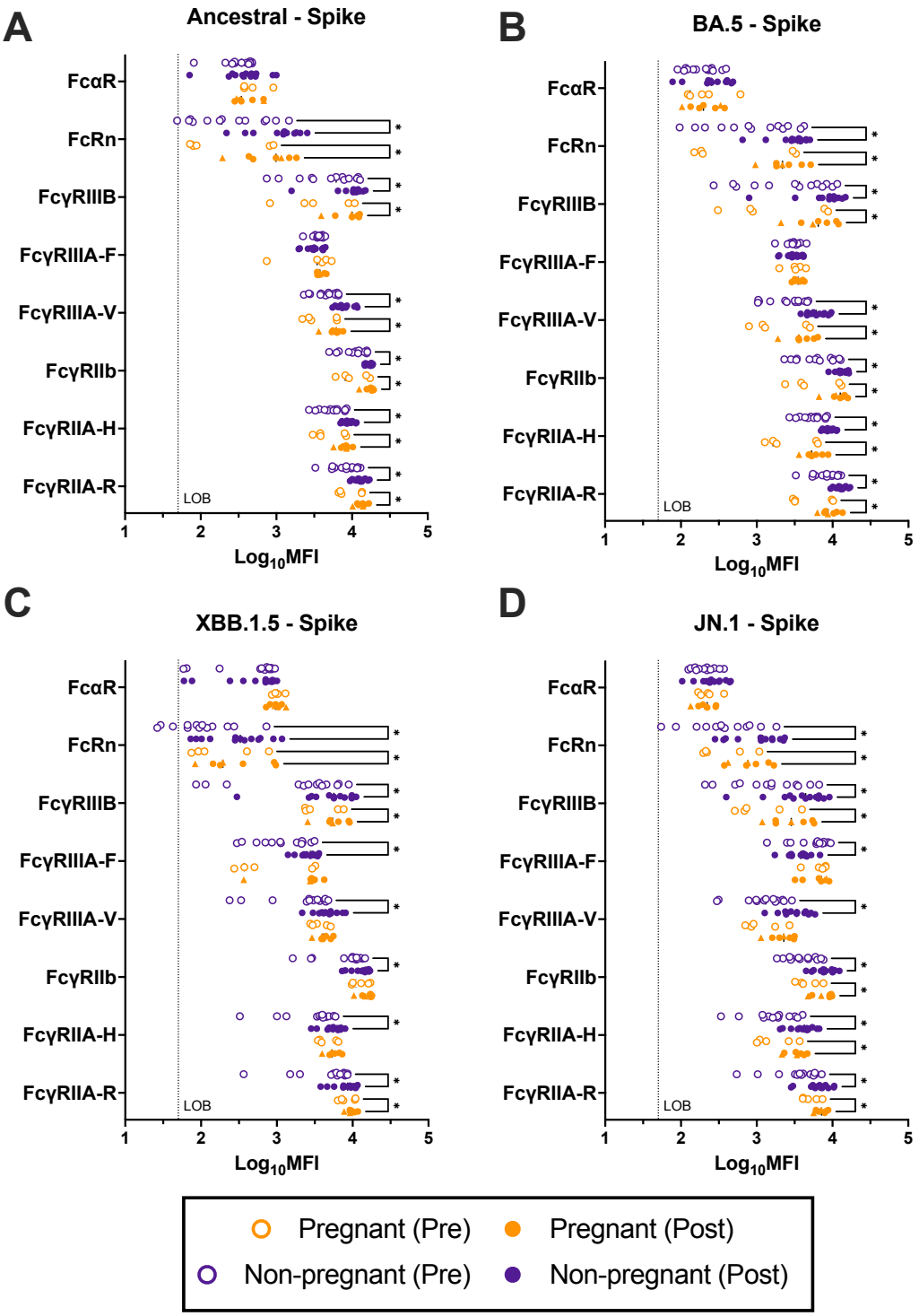

Figure 3. Fc receptor binding affinity is reduced in pregnant people in response to variants of concern. Serum antibody Fc receptor (FcR) binding affinity pre and 3-5 weeks post-vaccination were measured by multiplex Luminex bead assays and reported as $\log_{10}$ mean fluorescence intensity (MFI). Pregnant individuals (n=7) are shown in orange and non-pregnant females (n=13) in purple. Triangles highlight individuals who received monovalent boosters and circles represent bivalent booster recipients. Affinity for FcγRIIA-R, FcγRIIA-H, FcγRIIb, FcγRIIIA-V, FcγRIIIA-F, FcγRIIIB, FcRn, and FcαR was determined for **(A)** ancestral spike (S), **(B)** BA.5 S, **(C)** XBB.1.5 S, and **(D)** JN.1 S. Data were analyzed by linear mixed effects regression analysis with Bonferroni post-hoc. Asterisks indicate $p < 0.05$. Stippled line indicates limit of background (LOB) defined as the $\log_{10}$MFI of a defined negative control.

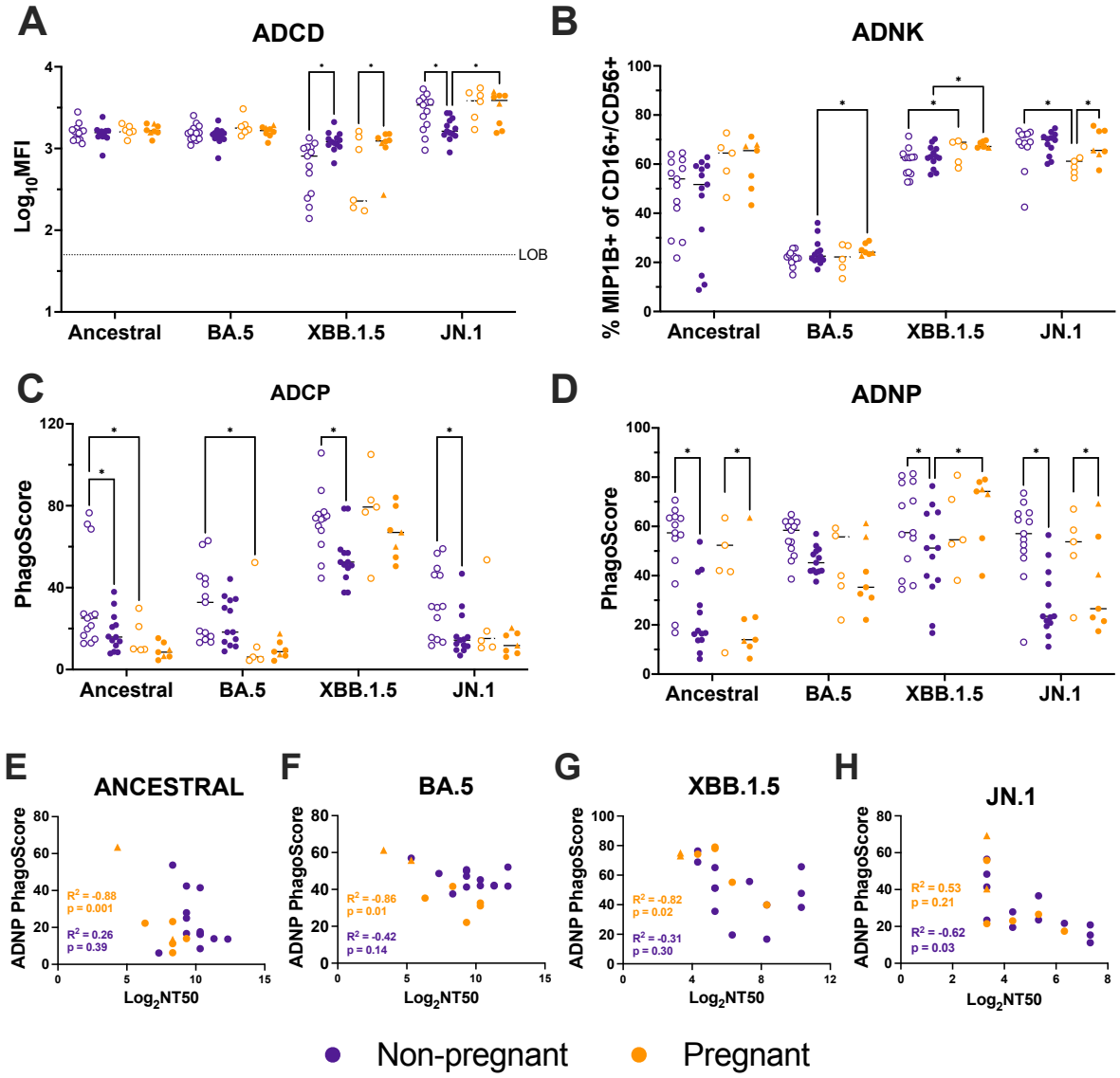

Figure 4. Non-neutralizing and neutralizing antibody functions are negatively correlated among pregnant individuals. Non-neutralizing antibody functions were measured pre and 3-5 weeks post-vaccination. Pregnant individuals (n=7) are shown in orange and non-pregnant females (n=13) in purple. Triangles highlight individuals who received monovalent boosters and circles represent bivalent booster recipients. **(A)** antibody dependent complement deposition (ADCD) was measured by assessing antibody affinity for C3 protein and is reported as $\log_{10}$ mean fluorescence intensity (MFI). Stippled line indicates limit of background (LOB) defined as the $\log_{10}$MFI of a defined negative control. NK cells isolated from donor blood were utilized to assess **(B)** antibody dependent NK cell cytotoxicity (ADNK), or the ability of antigen specific serum antibody to include NK cell cytokine production or degranulation. Data are reported as % MIP1B+ cells of CD16+/CD56+ NK cells. **(C)** THP-1 monocyte cell line was used to measure antibody dependent cellular phagocytosis (ADCP), or the ability of antibody to induce phagocytosis of antigen. **(D)** Neutrophils isolated from donor blood were used to measure antibody dependent neutrophil phagocytosis (ADNP), or the ability of antibody to induce neutrophil phagocytosis of antigen. ADCP and ADNP are reported as a PhagoScore, calculated as (% bead positive monocytes/neutrophils) * (geometric MFI of each cell). **(E-H)** Pearson correlations between neutralizing antibody titers (Log_2NT50) and ADNP PhagoScores for are shown for: **(E)** ancestral, **(F)** BA.5, **(G)** XBB.1.5, and **(H)** JN.1 viruses. Separate R2 and p-values are shown for each virus separated by pregnancy status. **(A-E)** Data were analyzed by linear mixed effects regression analysis with Bonferroni post-hoc. Asterisks indicate $p < 0.05$.

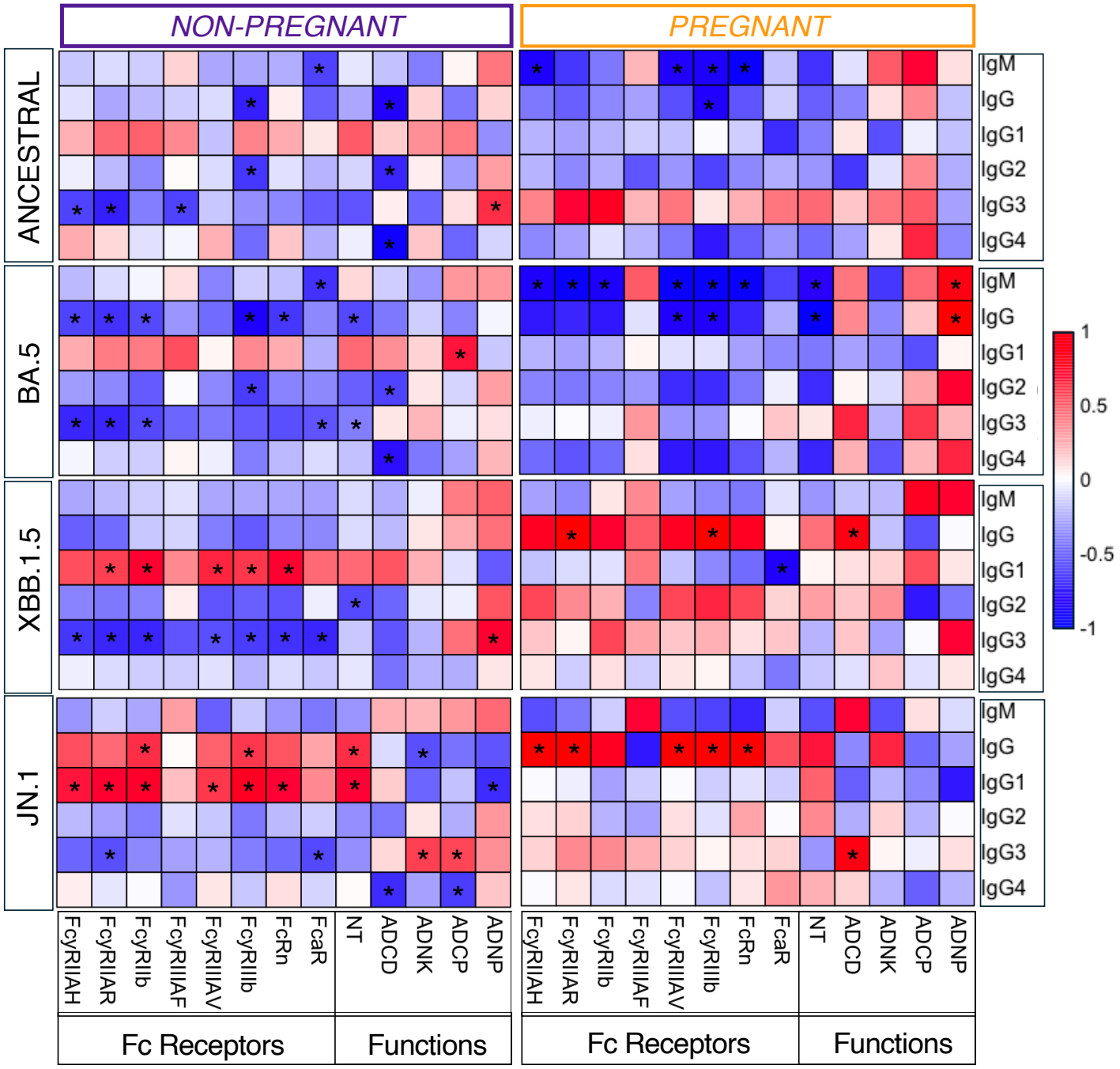

Figure 5. Correlations among IgG subclasses and antibody functional phenotypes differ between pregnant and nonpregnant individuals. Post-vaccination systems serology measures including isotype subclasses, FcR affinity, non-neutralizing functions, and neutralizing antibody (nAb) titers were $\log_{10}$ transformed and used for Spearman correlation analyses. Isotypes (y-axis) were correlated with functional measures (x-axis). Analyses were performed by pregnancy status. Asterisks indicate $p < 0.05$.

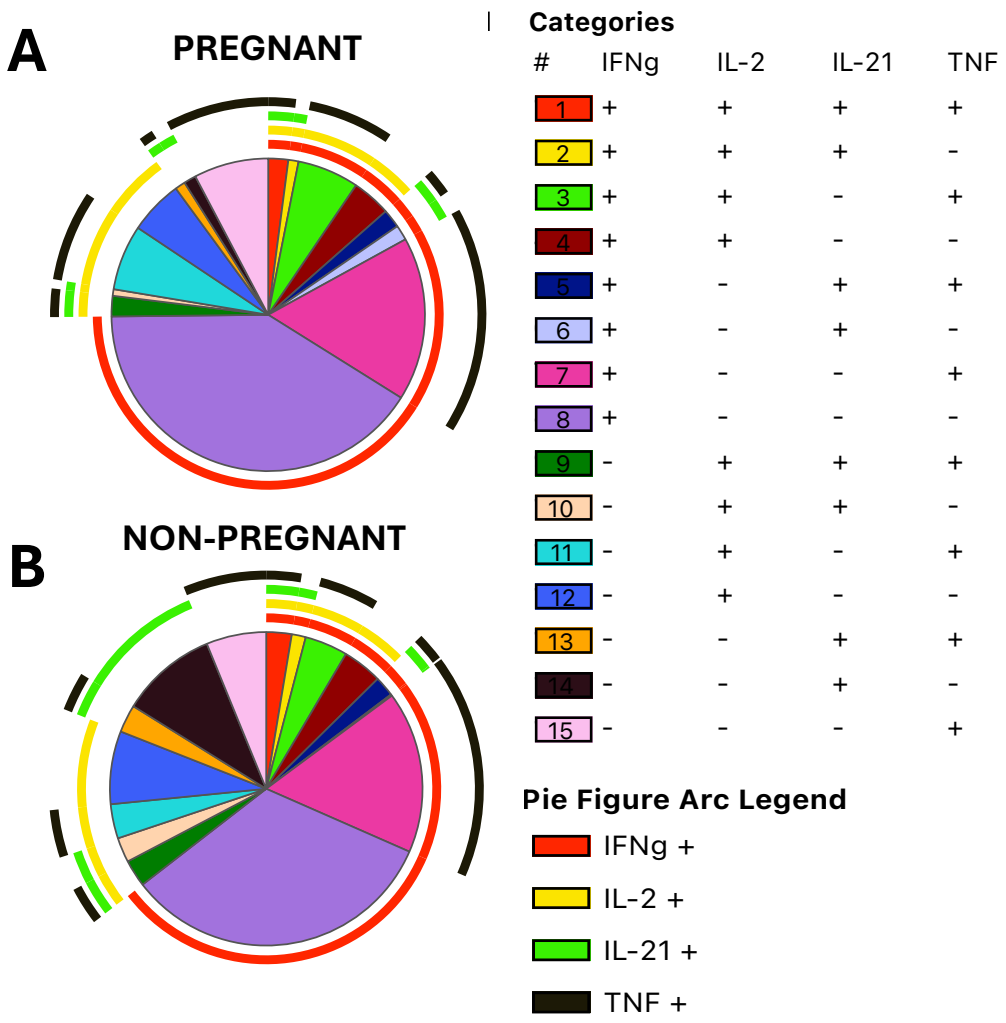

Figure 6. CD4+ T cells have reduced polyfunctionality among pregnant people. Peripheral blood mononuclear cells (PBMCs) were collected pre and 3-5 weeks post-vaccination for flow cytometry analyses. Cytokine-producing, antigen-specific CD4+T cells for **(A)** pregnant (n=7) and **(B)** non-pregnant (n=3) participants represented in pie charts broken down by the 15 cytokine combination categories. Arcs identify slices of the pie that express each specific cytokine**.** R values are shown for each correlation, and asterisks indicate $p < 0.05$.

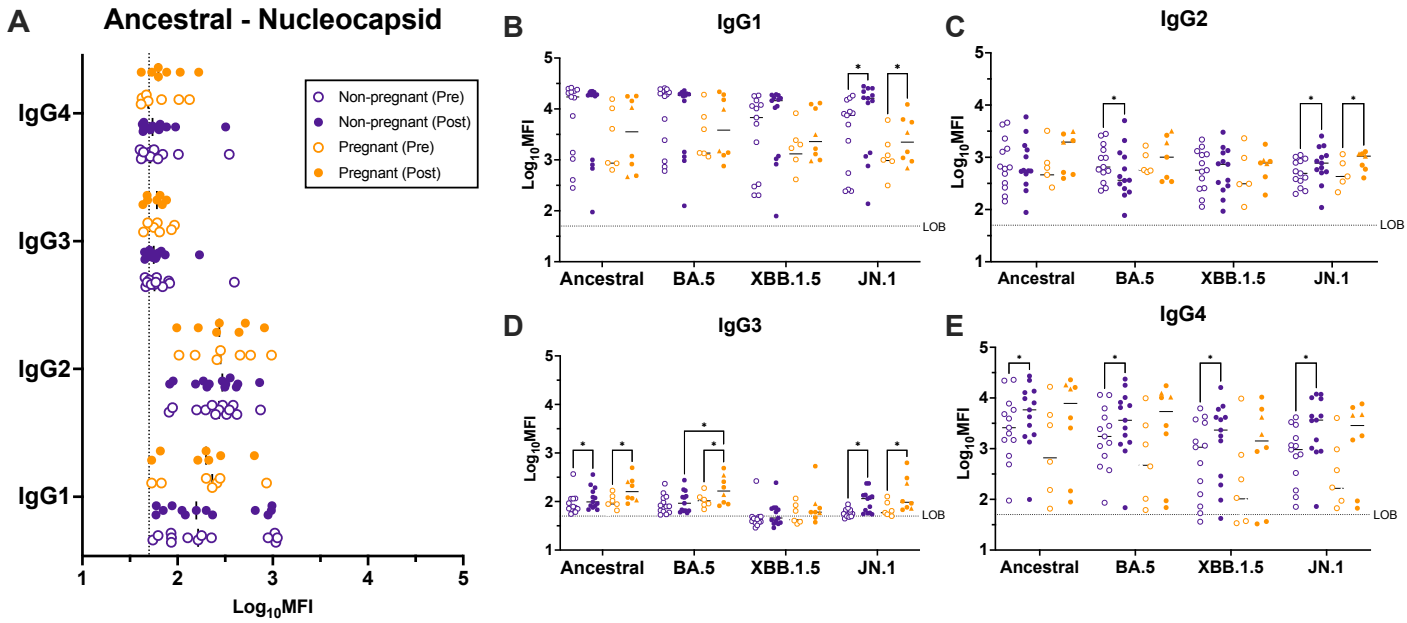

Supplemental Figure 1. Vaccination differently induces IgG subtype responses during pregnancy. IgG antibody responses in serum pre and 3-5 weeks post-vaccination were measured by systems serology and reported as $\log_{10}$ mean fluorescence intensity (MFI). Pregnant individuals (n=7) are shown in orange and non-pregnant females (n=13) in purple. Triangles highlight individuals who received monovalent boosters and circles represent bivalent booster recipients. **(A)** IgG subtype abundance to ancestral nucleocapsid (N) protein**.** IgG subtypes, including **(B)** IgG1 **(C)** IgG2, **(D)** IgG3, and **(E)** IgG4, in response to ancestral, BA.5, XBB.1.5, and JN.1 spike protein. Data were analyzed by linear mixed effects regression analysis with Bonferroni post-hoc. Asterisks indicate $p < 0.05$.

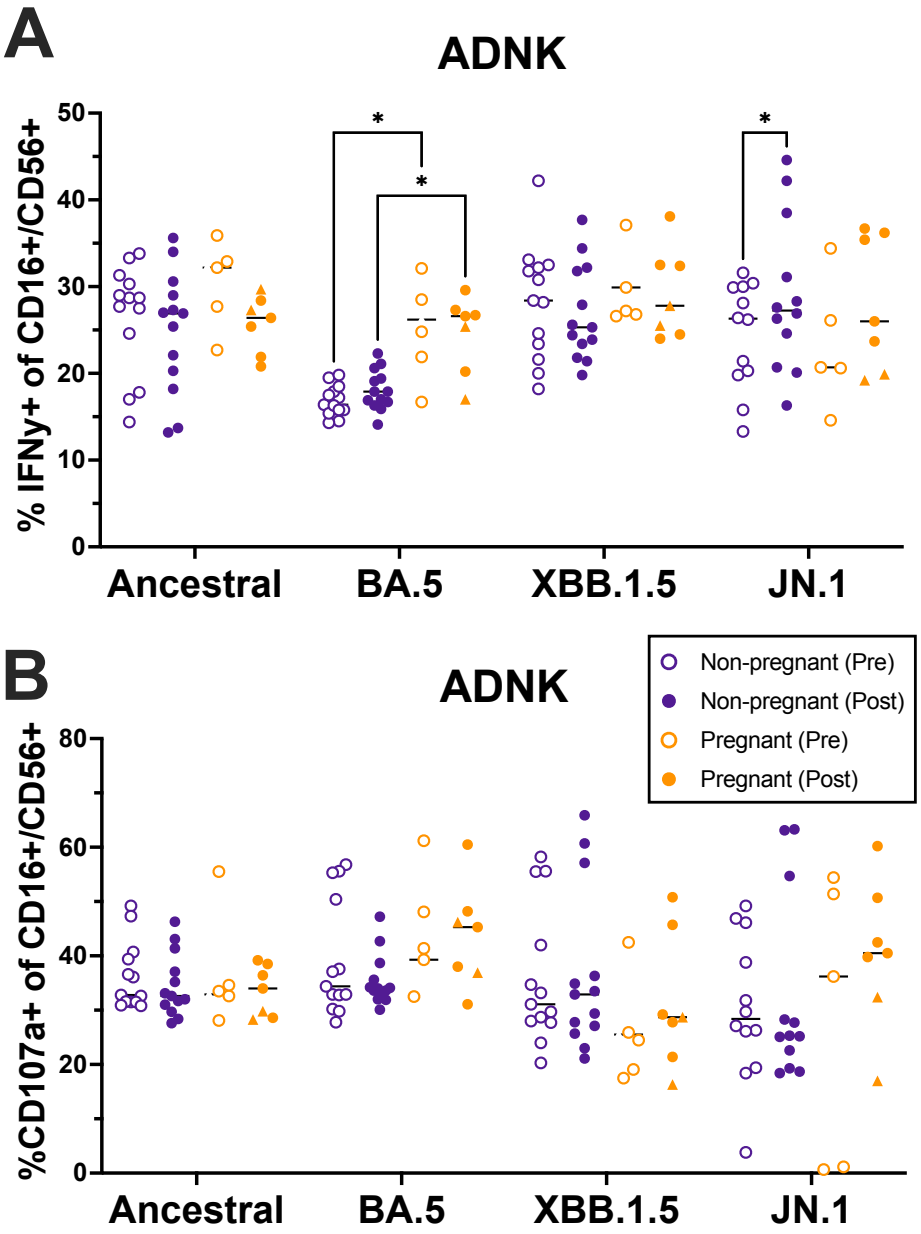

Supplemental Figure 2. Additional antibody-dependent NK cell responses by pregnancy status. NK cells isolated from donor blood were utilized to assess antibody dependent NK cell cytotoxicity (ADNK), or the ability of antigen specific serum antibody to include NK cell cytokine production or degranulation in serum pre and 3-5 weeks post-vaccination. Pregnant individuals (n=7) are shown in orange and non-pregnant females (n=13) in purple. Triangles highlight individuals who received monovalent boosters and circles represent bivalent booster recipients. ADNK was measured as ability to induce **(A)** IFNy production or **(B)** NK cell degranulation, as measured by CD107a positivity. Data were analyzed by linear mixed effects regression analysis with Bonferroni post-hoc. Asterisks indicate $p < 0.05$.

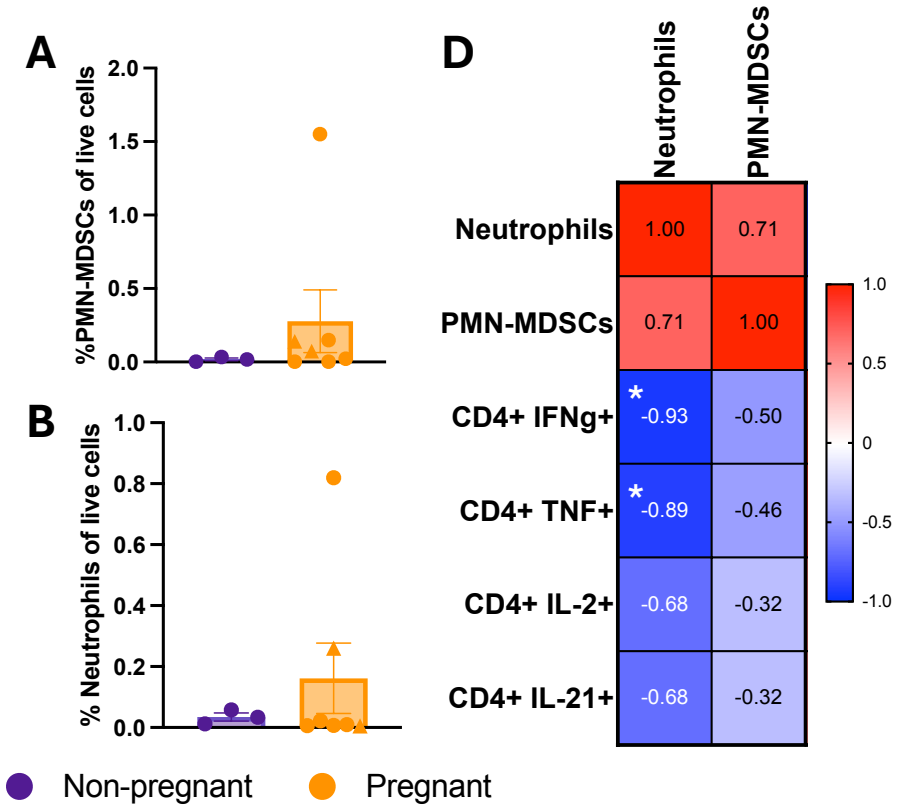

Supplemental Figure 3. Polymorphonuclear myeloid-derived suppressor cells correlate with CD4+ cytokine producing cells. Peripheral blood mononuclear cells (PBMCs) were collected pre and 3-5 weeks post-vaccination for flow cytometry analyses. Pregnant individuals (n=7) are shown in orange and non-pregnant females (n=3) in purple. Triangles highlight individuals who received monovalent boosters and circles represent bivalent booster recipients. **(A)** Neutrophils and **(C)** polymorphonuclear myeloid-derived suppressor cells (PMN-MDSCs) were quantified by flow cytometry and reported as a percentage of total live single cells. **(D)** Pearson correlations between cytokine producing CD4+ T cells, neutrophils, and PMN-MDSCs from pregnant people. R values are shown for each correlation, and asterisks indicate $p < 0.05$.

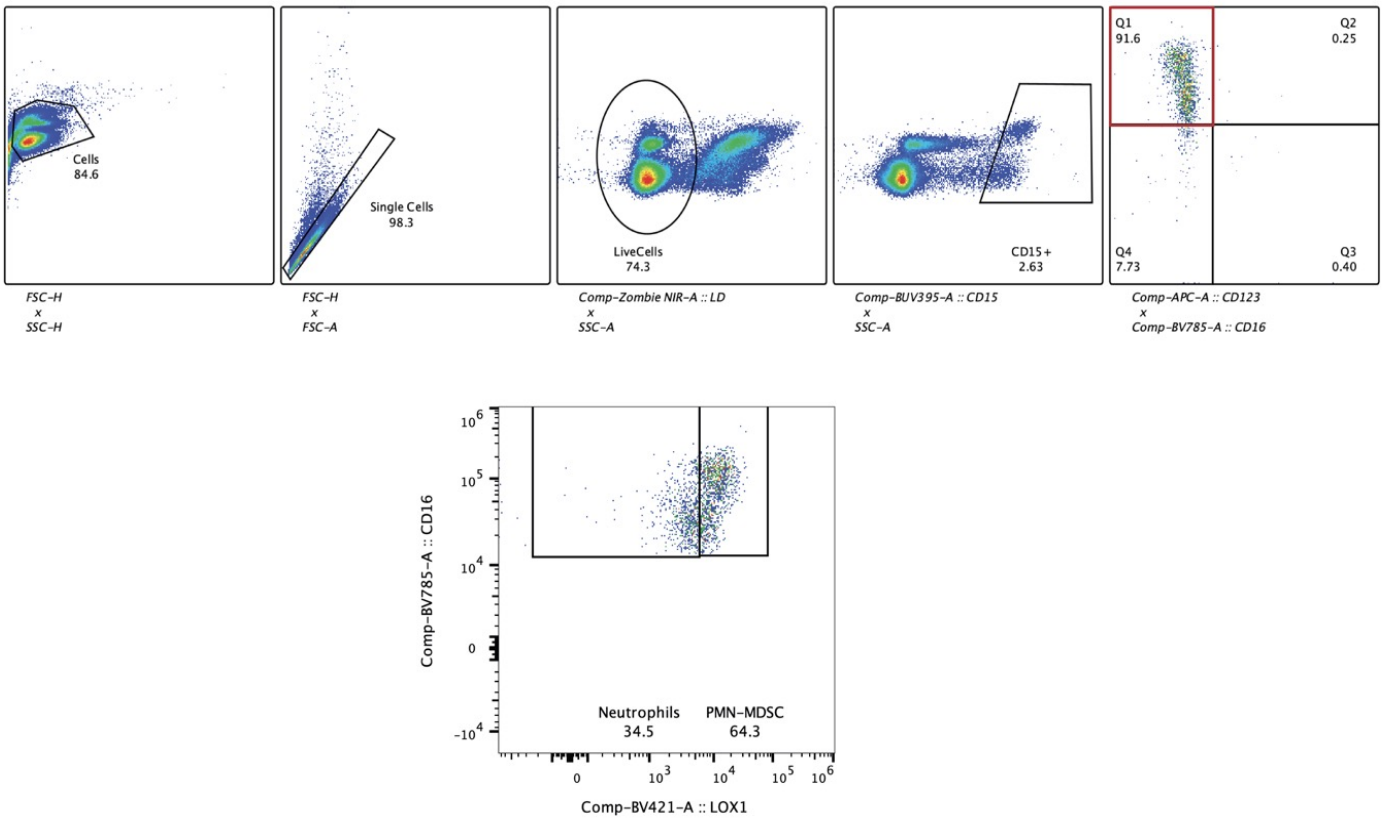

Supplemental Figure 4. PMN-MDSC gating strategy.

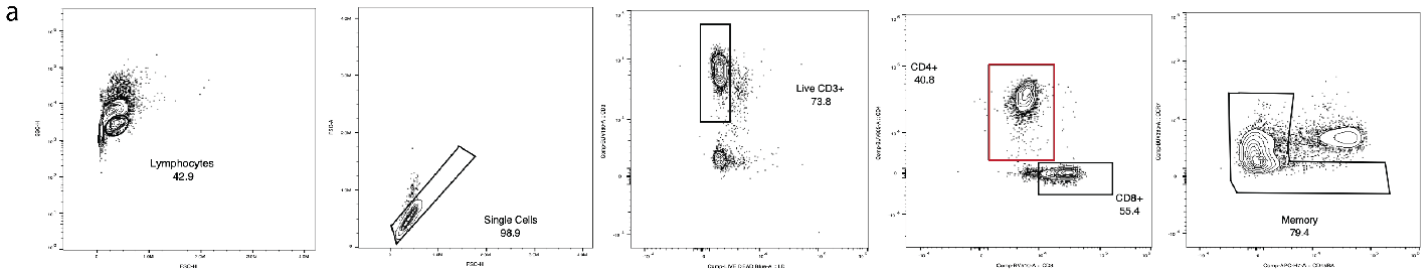

Supplemental Figure 5. Cytokine positive CD4+ T cells.

Supplemental Table 1A-B. Broad immune cell phenotyping (BIP) flow cytometry panel. (A) surface staining markers and **(B)** intracellular markers.

A. Surface

Fluorophore	Marker	Clone	Catalog	Vendor
BV570	CD33	WM53	303417	BioLegend
BV480	CD11c	B-ly6	566135	BD Biosciences
APC	CD123	6H6	306012	BioLegend
BV510	CD25	M-A251	563352	BD Biosciences
BV650	CCR7	G043H7	353234	BioLegend
BV421	LOX1	15C4	358610	BioLegend
BV711	CD38	HIT2	563965	BD Biosciences
APC-Cy7	CD19	SJ25C1	363010	BioLegend
APC-Cy7	CD56	5.1H11	362512	BioLegend
BV750	HLA-DR	L243	307672	BioLegend
BUV661	CD3	UCHT1	612964	BD Biosciences
BUV496	CD4	SK3	612936	BD Biosciences
BUV737	CD8	SK1	612754	BD Biosciences
BV785	CD16	3G8	302046	BioLegend
BUV805	CD14	M5E2	612902	BD Biosciences
BV605	CD86	BU63	374214	BioLegend
BUV563	CD45RA	HI100	612926	BD Biosciences
BUV395	CD15	H198	563872	BD Biosciences
Spark NIR	CD27	O232	302856	BioLegend
PE-Cy5	CD21	B-ly4	551064	BD Biosciences
PE-Cy5.5*	CD138	MI15	356502	BioLegend
PE-CF594	KLRG1	2F1	565393	BD Biosciences
BB790	IgD	IA6-2	BD Custom	BD Biosciences
BUV615	PD-1	EH12.1	612991	BD Biosciences

B. Intracellular

Fluorophore	Marker	Clone	Catalog	Vendor
Pacific Blue	FOXP3	206D	320116	BioLegend
PE-Cy7	Ki-67	Ki-67	350526	BioLegend
Alexa Fluor 488	CPT1a	8F6AE9	ab171449	Abcam
Alexa Fluor 680**	HK2	EPR20839	ab228819	Abcam
Alexa Fluor 532***	VDAC1	20B12AF2	ab14734	Abcam

Alexa Fluor 405	Tomm20	EPR15581-54	ab210047	Abcam
Alexa Fluor 647	GLUT1	EPR3915	ab195020	Abcam

Notes: * conjugated using PE/Cy5.5 Conjugation Kit - Lightning-Link (ab102899)

** conjugated using DyLight 680 Conjugation Kit (Fast) - Lightning-Link (ab201804)

*** conjugated using Alexa Fluor 532 Antibody Labeling Kit (Thermo Fisher, A20182)

Supplemental Table 2. Intracellular cytokine staining (ICS) flow cytometry panel. (A) surface staining markers and **(B)** intracellular markers.

A. Surface

Fluorophore	Marker	Clone	Catalog	Vendor
BUV395	CCR7	2-L1-A	749655	BD Biosciences
BV650	CXCR3	1C6	740603	BD Biosciences
PE CF594	KLRG1	2F1	565393	BD Biosciences
BV605	CD69	FN50	562989	BD Biosciences
BUV563	CD25	2A3	612918	BD Biosciences
BUV661	PD-1	EH12.1	750260	BD Biosciences
BUV737	TIM-3	7D3	748820	BD Biosciences
BV570	CD28	CD28.2	302926	Biolegend
PE Cy5	CD127	HIL-7R-M21	BD Custom	BD Biosciences
BUV805	CD4	SK3	612887	BD Biosciences
APC H7	CD45RA	HI100	560674	BD Biosciences
BB660	Tigit	741182	BD Custom	BD Biosciences
BV711	OX40	ACT35	563664	BD Biosciences
BV786	CD27	L128	563327	BD Biosciences
PE Cy7	CTLA-4	BNI3	BD Custom	BD Biosciences
BV510	CD8a	HIT8a	300934	Biolegend
BB790	CXCR5	RF8B2	BD Custom	BD Biosciences

B. Intracellular

Fluorophore	Marker	Clone	Catalog	Vendor
PE	IL-21	3A3-N2	513004	BioLegend
AF680**	HK2	EPR20839	ab228819	Abcam
AF488	TCF1	812145	IC8224G	FisherScientific
BV421	IL-2	MQ1-17H12	564164	BD Biosciences
AF532***	VDAC1	20B12AF2	ab14734	Abcam

BV750	TNF	MAb11	566359	BD Biosciences
PECy5.5*	CPT1a	8F6AE9	ab128568	Abcam
AF405	Tomm20	EPR15581-54	ab210047	Abcam
Alexa647	GLUT1	EPR3915	ab195020	Abcam
BUV496	CD3	UCHT1	612940	BD Biosciences
BB700	IFNy	B27	566394	BD Biosciences

Notes: * conjugated using PE/Cy5.5 Conjugation Kit - Lightning-Link (ab102899)

** conjugated using DyLight 680 Conjugation Kit (Fast) - Lightning-Link (ab201804)

*** conjugated using Alexa Fluor 532 Antibody Labeling Kit (Thermo Fisher, A20182)